

Imperial College London
Department of Theoretical Physics

On the Classification of Brane Tilings: Expanded

Jurgis Pasukonis

September 25, 2009

Supervised by Amihay Hanany

Submitted in part fulfilment of the requirements for the degree of
Master of Science in Theoretical Physics of Imperial College London

Abstract

We present a computationally efficient algorithm that can be used to generate all possible brane tilings. Brane tilings represent the largest class of superconformal theories with known AdS duals in 3+1 and also 2+1 dimensions and have proved useful for describing the physics of both D3 branes and also M2 branes probing Calabi-Yau singularities. This algorithm has been implemented and is used to generate all possible brane tilings with at most 6 superpotential terms, including consistent and inconsistent brane tilings. The collection of inconsistent tilings found in this work form the most comprehensive study of such objects to date.

This paper is an expanded version of hep-th/0909.2868, with the same key results, but a more thorough presentation of the background material.

Acknowledgements

I am very grateful to my thesis supervisor Amihay Hanany, and John Davey with whom this project was carried out. I would like to thank Benjo Fraser, Mike Delph and James McHugh for many enlightening discussions. I also thank Stefano Orani and Dionigi Benincasa for warm encouragement and support.

Contents

1. Introduction	5
2. Background	8
2.1. AdS/CFT	8
2.2. Quivers	11
2.2.1. $\mathcal{N} = 1$ quiver gauge theory in 3+1	11
2.2.2. $\mathcal{N} = 2$ quiver Chern-Simons theory in 2+1	15
2.3. Brane Tilings	17
2.4. Moduli space calculations	21
2.4.1. Toric geometry	21
2.4.2. Forward algorithm	22
2.4.3. Extra consistency conditions	24
3. Classification Algorithm	26
3.1. Motivation	26
3.2. Method Overview	27
3.3. The Doubling Process and Quadratic-Node Tilings	28
3.4. Algorithm in detail	30
3.4.1. Order parameters	30
3.4.2. Finding Quivers	32
3.4.3. Finding Superpotentials	33
3.4.4. Reconstructing Tilings	34
4. Result Overview	38
5. Conclusions	42
A. Appendix: Tiling catalog	44
A.1. Two superpotential terms	44
A.2. Four superpotential terms	44
A.3. Six superpotential terms	47

1. Introduction

Ever since the discovery of the AdS/CFT correspondence there has been a tremendous amount of ongoing activity in exploring the consequences of this duality. One of the directions of research has been to find explicit Lagrangian descriptions of field theory duals to various AdS backgrounds. An archetypical example of such explicit correspondence is the $AdS_5 \times S^5$ dual to the $\mathcal{N} = 4$ SYM theory.

Probably the largest class of backgrounds with known Lagrangian descriptions of CFT duals is the $AdS_5 \times X_5$ where X_5 is a Sasaki-Einstein manifold and the cone over X_5 is a *toric* Calabi-Yau. Such backgrounds are dual to a world-volume theory of a stack of D3 branes probing the Calabi-Yau. It can be shown that the D3 world volume theory can be completely described by a structure known as brane tiling, representing a T-dual configuration of D5 and NS5 branes. The brane tiling then also encodes a Lagrangian of a (3+1)-dimensional $\mathcal{N} = 1$ quiver gauge theory. Thus using the framework of brane tilings there is by now a well established way to construct a $\mathcal{N} = 1$ CFT Lagrangian for any background toric Calabi-Yau threefold [2, 3]. These methods are reviewed in [4, 5].

Recently there has been a lot of activity regarding the Lagrangian description of M2 brane world-volume theories, started by [6, 7]. It was then found that the theory on an M2 brane in flat spacetime can be described by an $\mathcal{N} = 6$ (2+1)-dimensional quiver Chern-Simons theory [8]. This was followed by an observation that the same brane tiling models used to describe D3 brane theories can be used to construct a whole class of $\mathcal{N} = 2$ (2+1)-dimensional quiver Chern-Simons Lagrangians, that have an 8-dimensional toric Calabi-Yau moduli space Y_8 , indicating a world-volume theory of an M2 brane probing a Y_8 instead of a flat spacetime [9, 10].

These advances have led to a conjecture that the brane tilings might again provide a framework to construct explicit Lagrangians for CFT duals to a new infinite class of $AdS_4 \times X_7$ backgrounds, where the cone over X_7 is a toric Calabi-Yau Y_8 , as they are believed to correspond to world-volume theories on M2 branes probing the Y_8 . The situation here, however, is much less clear compared to the (3+1)-dimensional story. So far the main tool for exploring

this correspondence has been the calculation of Y_8 toric moduli space for a given tiling, a procedure called the “Forward Algorithm” [10, 11]. This gives a candidate Lagrangian description of the Y_8 background, on which then further consistency checks should be performed. The problem is that so far there are no universal consistency checks available, to pick out a preferred SCFT dual from the candidates. An analogous consistency check in the (3+1)-dimensional case does exist and provides the class of “consistent tilings”. Another problem is that unlike for the $AdS_5 \times X_5$ backgrounds, here we do not have an “inverse algorithm”, which would construct the dual tiling given any Y_8 of interest, which is ultimately the desired result.

Given these new problems in the M2 brane case, a systematic study of the possible toric quiver Chern-Simons theories was initiated in [11]. Here we proceed in the spirit of that work with the systematic study of brane tilings. Specifically, we propose an efficient algorithm which can, in principle, generate all brane tilings up to desired complexity, and calculate their moduli spaces. We use an implementation of the algorithm to generate the tilings with up to six nodes. We find that the list includes the consistent tilings which have already been analyzed in the context of D3 brane theories and also a large number of so far undiscovered “inconsistent” models. These are known to not describe a consistent (3+1)-dimensional CFT, but they might well prove useful in providing M2 world-volume Lagrangians.

The motivation for the work is the following. First, with the absence of the inverse algorithm, the only universal way to find the tiling dual to a given Y_8 background is to scan through the possible tilings, until we find one with the moduli space that we are looking for. In this work we propose an exact algorithmic solution for just that. Another motivation is a hope, that in the list of possible tilings with their associated moduli spaces some patterns would emerge, which would provide additional insights into possibilities and limitations of the tiling framework, and its applicability to describe M2 world-volume theories. Even in the context of D3 brane theories, though many tilings were constructed for specific cases, there is as of now no complete classification of the models. Here we provide such a list up to certain level of complexity. Finally, there is a pure curiosity in systematically exploring the rich space of geometrical structures of tilings.

The paper is organized as follows. In Chapter 2 we provide the reader with the background to better understand both the motivation and the details of the problem associated with the brane tilings. First we introduce some main facts regarding the AdS/CFT correspondence. Then we describe the role of

the quiver gauge theories in this context, and how they can be used to provide Lagrangians for both D3 and M2 world-volume field theories. Afterwards we arrive at the concept of tilings, discuss how they are related to quiver gauge theories, and how to perform calculations of the vacuum moduli space. Chapter 3 proceeds to a detailed description of the proposed algorithm to generate the possible tilings. An implementation of the algorithm is used to generate all tilings of up to six nodes, which are presented in the catalog in Appendix A. These results are discussed in Chapter 4. Finally, we end with conclusions and discussion of the possible further work.

Note that this paper is an expanded version of [1], which also contains all the main results presented here.

2. Background

2.1. AdS/CFT

In this work we are interested in exploring a class of dualities of the AdS/CFT type, so let us first give some basic background regarding the correspondence. It is by now a well established conjecture, that a quantum gravity theory (such as string theory or M-theory) on $AdS_d \times X_n$ background is dual to some conformal field theory (CFT). Here AdS_d is a d -dimensional Anti de Sitter spacetime and X_n is an internal compact manifold. In addition the background can contain fluxes of some of the fields. The dual CFT then lives on a $(d - 1)$ -dimensional space, but the exact theory depends on the details of the background, specifically, on the X_n space and the fluxes. The problem that we are interested in here is how, given a particular background, we can write the exact Lagrangian for the dual CFT.

Even though the dual CFT is supposed to exist for any background, there are in the most general case no rules of writing a Lagrangian for the dual field theory. There are, however, classes of backgrounds for which the precise construction of the dual CFT is known, and we examine some of these cases in this work. In particular, we are interested in two types of backgrounds: the Type IIB string theory on $AdS_5 \times X_5$ and the M-theory on $AdS_4 \times X_7$. The internal manifold X_n in both cases is a Sasaki-Einstein manifold¹. In addition we have to specify that all the field fluxes in the background are zero, except the 5-form field strength in the $AdS_5 \times X_5$ case and the 7-form field strength in the $AdS_4 \times X_7$ case, which have a flux N on the internal X_n manifold.

The gravity background for this class of theories is thus specified by the X_n and number N and we want to see if we can find the explicit Lagrangian description of the dual CFT. Let us first concentrate on the $AdS_5 \times X_5$ case in Type IIB, which is dual to a 4-dimensional CFT. This is the well-known class of AdS_5/CFT_4 dualities, with the archetypical example of the $AdS_5 \times S^5$ duality to the $\mathcal{N} = 4$ Super Yang-Mills (SYM) theory in 4 dimensions and gauge group

¹“Sasaki-Einstein” means that the manifold has some special “nice” properties, but it is not too restrictive, and so the class of such manifolds is still very wide with several infinite families known explicitly

$SU(N)$.

The crucial observation, that helps to establish the AdS/CFT correspondence, is that the $AdS_5 \times S^5$ spacetime with the 5-form flux N can be seen as arising near the horizon around a stack of N D3 branes placed in a *flat* 10-dimensional spacetime. Then in a certain limit one can see, that the same near-horizon physics can be described either by a gravity theory on the $AdS_5 \times S^5$ or by a *world-volume field theory* of the stack of D3 branes. And the world-volume theory of D3 branes in flat spacetime is known to be the $\mathcal{N} = 4$ SYM.

This construction can be generalized to X_5 manifolds other than S^5 [12, 13, 14, 15]. In order for general $AdS_5 \times X_5$ near-horizon geometry to arise, it turns out that the stack of D3 branes has to be placed not in a flat space, but in a $\mathbb{R}_{3,1} \times Y_6$, where $\mathbb{R}_{3,1}$ is a flat Minkowski spacetime and Y_6 is a cone over X_5 :

$$Y_6 = C(X_5). \quad (2.1)$$

By a “cone over a manifold” we mean that we add an extra radial coordinate $r \geq 0$ and we take X_5 do be the “angular” part of the coordinates at each r , so that topologically $C(X_5) = \mathbb{R}^+ \times X_5$ and the metric is

$$ds_{C(X)}^2 = dr^2 + r^2 d\Omega_X^2. \quad (2.2)$$

Let us note a few things about the Y_6 space. First, while X_5 is compact, Y_6 is non-compact, since it now has an infinite radial coordinate. For example, if $X_5 = S^5$ like in the SYM case, then the angular S^5 coordinate together with r just provides the usual spherical coordinates, and so $Y^6 = C(S^5) = \mathbb{R}_6$ is just the 6-dimensional flat space. Second, the fact that X_5 is a Sasaki-Einstein implies that Y_6 is a Calabi-Yau space², which can also be seen as a complex 3-manifold CY_3 . And third, for arbitrary X_5 the point at $r = 0$ actually turns out to be singular. This can intuitively be seen by picturing the Y_6 as an actual cone, with r specifying the distance from the tip of the cone. If then the remaining space for each r is not symmetric enough (like S^5), the tip of the cone itself (at $r = 0$) will not be smooth.

The singularity at $r = 0$ of Y_6 is the crucial point, though. In order to create the $AdS_5 \times X_5$ geometry as promised, we have to place the stack of D3 branes in $\mathbb{R}_{3,1} \times Y_6$ in such a way that they span the 4-dimensional Minkowski space and are transverse to the Calabi-Yau space. Moreover, the position of the branes on the Y_6 has to be exactly at the singularity $r = 0$, so that they can “see” the full geometry (if the D3 branes were placed somewhere else on Y_6 , they would

²Again, that means that it has some special “nice” properties

only see local geometry, which would be \mathbb{R}_6 and it would result in the same dual $\mathcal{N} = 4$ SYM). This configuration is often referred to as “D3 branes probing a Calabi-Yau singularity”.

Given that we now have a configuration of D3 branes that creates the desired spacetime geometry, we can expect that it is the world-volume theory on the branes that gives the dual CFT to the gravity in spacetime. The question is then how we can find the explicit Lagrangian for the theory. There are a few general features that one can expect from a candidate dual field theory. First, we want the QFT specified by the dual Lagrangian to flow to a conformal fixed point in the IR limit [24, 25]. This requirement arises from a more careful analysis of the AdS/CFT correspondence, which is roughly as follows. The world-volume Lagrangian for the D3 branes that we write down is considered to specify the “UV theory”, which is not necessarily conformal, and not exactly dual to the Type IIB string theory on $AdS_5 \times X_5$. It is in the near-horizon limit that the duality is manifest, and that corresponds to going to the IR limit of the world-volume field theory. Thus we have to require that the field theory with the specified UV Lagrangian flows to an IR fixed point, where it is conformal, and dual to the Type IIB string theory on $AdS_5 \times X_5$ background.

Another property that the dual Lagrangian has to have concerns the space of possible vacuum configurations, i.e. the moduli space. When D3 branes are placed transverse to the Calabi-Yau space, there must be scalar degrees of freedom living on the world-volume, that parametrize the positions of the D3 branes on Y_6 . These scalar degrees of freedom can acquire VEVs, which make up the moduli space. If we have only one D3 brane probing the Calabi-Yau, then the vacuum should be described by VEVs of exactly 6 fields, and so the moduli space should be the Y_6 itself! In general, with N branes, in order to specify vacuum positions we need $6N$ coordinates, but we have to divide by the permutation of identical branes, so the moduli space has to be

$$\mathcal{M} = (Y_6)^N / S_N \tag{2.3}$$

where S_N is the permutation group.

These properties already give us a clue how to look for the dual CFT. Given a 4-dimensional Lagrangian it is usually not too difficult to calculate the resulting moduli space \mathcal{M} of the theory (the procedure is called the “Forward Algorithm” in the context of this work). If we find that \mathcal{M} indeed corresponds to Y_6 that we are interested in, it is already a good guess for the dual theory. Then one can proceed with further checks, such as the flow to IR conformal fixed point, calculation of R -charges, etc, in order to confirm the duality. To proceed with

this search, however, we need some guidelines on what form of Lagrangians to consider.

A large class of field theories that proved to be good candidates for the AdS_5/CFT_4 duality are the so-called “quiver gauge theories”. We describe them in Section 2.2 and show some examples. It is also known that the CFT consistency checks put further restrictions on the allowed Lagrangians, that refine the models of interest to a *subset* of the quiver gauge theories known as “brane tilings” [2, 3]. We describe these theories in detail in Section 2.3. It is precisely this class of dual CFTs arising from brane tilings, that is the central interest of this work.

The discussion in this section so far was considering Type IIB string theory on $AdS_5 \times X_5$ as a background, but, as mentioned, we are also interested in analysing the M-theory on $AdS_4 \times X_7$. Such theory should be dual to a CFT in 2+1 dimensions. Here the duality can be constructed in a similar way, by considering a stack of M2 branes at the tip of a Calabi-Yau Y_8 , which is a cone over X_7 . The dual CFT should then arise as a world volume theory on M2 branes. The problem with this duality until recently was that there was no satisfactory Lagrangian description of the world-volume theory of M2 branes. However, with recent advances in this area [6, 7, 8] it was realized that 2+1 dimensional Chern-Simons Lagrangian can do the job. Even though in this case the full picture of the duality is much less clear than with D3 branes, we can begin by again calculating the moduli spaces and comparing them with the Y_8 , thus finding the candidate dual theories. It turns out that quiver gauge theories and brane tilings again provide a large class of Lagrangians, which are potentially dual to various X_7 backgrounds [9, 10]. It is in this context that the current work might be most useful.

2.2. Quivers

In this section we explain quiver gauge theories and how they can be used to describe both world-volume theory on D3 branes and on M2 branes. In the next section we refine the discussion to the case of brane tilings, which in this context constitute the most interesting subset of quiver gauge theories.

2.2.1. $\mathcal{N} = 1$ quiver gauge theory in 3+1

Let us again concentrate on the world-volume theory on D3 branes first. In Section 2.2.2 we will show how the same structure can be carried over to the case of M2 branes.

In order to define a gauge field theory in general we need to specify two things: the gauge group g and the matter fields Φ_A together with their representation under g . In addition, there might be a potential for the scalar fields in the theory. The *quiver* gauge theories are then characterized by the following properties. First, the gauge group g has to be a product of a number of $U(N)$ groups³:

$$g = U(N) \times U(N) \times \dots \times U(N). \quad (2.4)$$

We refer to i 'th $U(N)$ group factor as the i 'th gauge group or g_i . Second, the matter fields have to transform as *bifundamental* or *adjoint* representations under the group factors. Bifundamental representation means that the field has a fundamental representation under one of the groups g_i and anti-fundamental under another group g_j , and we usually denote such matter field as X_{ij} . We can actually then view each bifundamental matter field as a matrix $(X_{ij})_{a\bar{b}}$ where index a transforms fundamentally under g_i and \bar{b} transforms anti-fundamentally under g_j . Alternatively, a matter field can be adjoint under one of the groups g_i , which we denote by Φ_i . This again can be seen as a matrix $(\Phi_i)_{a\bar{b}}$, where both indices transform under g_i .

The bifundamental (or adjoint) nature of the fields allows for a particularly convenient way to represent the gauge group and the matter multiplet: it can be seen as a *oriented graph*, where each group factor is represented by a node, and each matter field X_{ij} by an arrow going from node i to j . This graph is called a “quiver diagram”, and that is where the “quiver” name comes from, since the fields are represented by a collection of arrows. We usually refer to the diagram as just the “quiver”. In Figure 2.1 we give an example of a quiver with group $g = U(N) \times U(N) \times U(N)$ and six bifundamental matter fields plus one adjoint matter field.

In the case of the world-volume theories on D3 branes we have Lagrangians which have $\mathcal{N} = 1$ supersymmetry in four spacetime dimensions. This comes from the fact that the dual $AdS_5 \times X_5$ space preserves 8 supercharges when X_5 is Sasaki-Einstein. The matter fields in the quiver X_{ij} and Φ_i then correspond to *chiral multiplets*, containing a spin-1/2 particle and a complex scalar.

Because $\mathcal{N} = 1$ supersymmetry and the gauge group does not fully specify the Lagrangian in four spacetime dimensions, we need one extra piece of information to define a gauge theory: the superpotential W .⁴ The Lagrangian is then of

³The definition could be more general, allowing the group factors have different ranks and/or be $SU(N)$, $Sp(N)$ or $SO(N)$ rather than $U(N)$, but we restrict ourselves to this simplest definition.

⁴Note that the case when $X_5 = S^5$ is special in that it has a maximal amount of supersymmetry, leading to a $\mathcal{N} = 4$ supersymmetry in (3+1)-dimensions, which uniquely determines

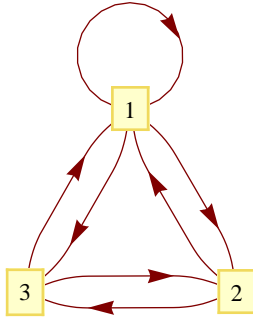


Figure 2.1.: Example of a quiver with six bifundamental ($X_{12}, X_{21}, X_{23}, X_{32}, X_{31}, X_{13}$) and one adjoint (Φ_1) fields.

the form:

$$\mathcal{L}_4 = \text{Tr} \left(\int d^4\theta \sum_{X_{ij}} X_{ij}^\dagger e^{-V_i} X_{ij} e^{V_j} + \int d^2\theta \mathcal{W}^\alpha \mathcal{W}_\alpha + \int d^2\theta W(X_{ij}) + \text{c.c.} \right). \quad (2.5)$$

We can initially consider the superpotential to be any gauge invariant polynomial of the matter fields. In order to construct gauge invariant terms we can simply contract fundamental indices with the anti-fundamental, thus producing terms of the form

$$\text{Tr} (X_{ij} X_{jk} X_{kl} \dots X_{ri}), \quad (2.6)$$

where the multiplication between fields is a matrix multiplication, and the adjacent group labels match (note that it is not the indices i, j, k, \dots that are contracted, they just have to be the same!). Now such gauge invariant products have a nice representation in the quiver diagram: the arrows have to be contracted head-to-tail and so the product has to be a *closed loop* in the graph. The full superpotential is a sum of such terms, so for example in Figure 2.1 it could be

$$W = \text{Tr} (\Phi_1 X_{12} X_{21} - \Phi_1 X_{13} X_{31} + X_{13} X_{32} X_{23} X_{31} - X_{12} X_{23} X_{32} X_{21}) \quad (2.7)$$

(it could be many other things as well, we explain shortly why we like this particular superpotential for that quiver).

Given a quiver and a superpotential, we can go and calculate the moduli space, hoping to find the dual Calabi-Yau. In general, given an $\mathcal{N} = 1$ supersymmetric gauge theory, the vacuum configurations are found by solving the

the Lagrangian.

so-called F-term and D-term constraints. It is easiest to analyze them in the case of world-volume theory on a single D3 brane. Then the group factors are $U(1)$ and the fields are just number-valued. More importantly, the moduli space should be just Y_6 . The F-terms depend on the superpotential W and require for each matter field X_A that:

$$\frac{\partial W}{\partial X_A} = 0. \quad (2.8)$$

The D-terms depend only on the representations of the fields and require for each gauge group g_i :⁵

$$\sum_A d_{iA} |X_A|^2 = 0. \quad (2.9)$$

The charges d_{iA} are (+1) if field X_A is fundamental under g_i and (-1) if anti-fundamental, otherwise zero.

The system of algebraic relationships between complex fields X_A given by F-terms and D-terms defines a space of solutions which we want to look like a Calabi-Yau singularity. In algebraic geometry such space is what is called an algebraic variety, and we might look there for some general tools to solve our problem. It turns out that for the most general case of Calabi-Yaus we can not say much, but there is a special subclass of them called *toric Calabi-Yau* spaces, which we can analyze in great detail using the language of *toric geometry*.

The condition that we want the algebraic variety defined by F-terms and D-terms to be a *toric* Calabi-Yau enforces a strict condition on the form of W . It states that each matter field should only appear in the superpotential *twice*: once in a positive term and once in a negative term. One can see, for example, how that is satisfied in (2.7). That means that from the perspective of any field X_A the superpotential looks like:

$$W = X_A \times P(X) - X_A \times R(X) + (\text{other terms}), \quad (2.10)$$

where $P(X)$, $R(X)$ are monomials of fields not including X_A and other terms don't depend on X_A . Therefore all the F-terms are of the form

$$P(X) = R(X), \quad (2.11)$$

a relationship between two monomials. We refer to this restriction on the superpotentials as *toric condition*

There is one other restriction that we have to enforce on the quivers. In

⁵Here we take the so-called FI parameters ζ^i to be zero, which corresponds to “unresolved” singular Calabi-Yau Y_6 .

general, a quiver gauge theories contains anomalies when quantized because of the presence of chiral fields. In order for the anomalies to cancel, it turns out that we need the total charge under each group to be zero [3]:

$$\sum_A d_{iA} = 0, \quad \forall i. \quad (2.12)$$

From the point of view of the quiver, this implies that *each group node has to have the same number of incoming and outgoing arrows*.

Given an $\mathcal{N} = 1$ quiver gauge theory with these two conditions there is, in fact, a completely determined procedure to solve the F- and D-terms and calculate the resulting toric Calabi-Yau space, described by an object called *toric diagram*. This procedure is called the ‘‘Forward Algorithm’’ [10, 11] and is described in Section 2.4. Using it we could already start a systematic search for dualities. We could, in principle, examine all possible quivers with the anomaly cancellation condition in increasing complexity. For each quiver then there is only a finite number of possible superpotentials constrained by the toric condition. By calculating the moduli space for each of the models, we can find a set of potentially dual quiver gauge theories for each resulting Y_6 .

However, many of the gauge theories constructed this way still fail to be consistent CFT duals, satisfying the flow to IR and other conditions. It would be nice then to have some further restrictions on the quiver gauge theories, that would indicate the best candidates for dualities. It turns out that there is such a restriction, and it provides a subset of quiver gauge theories called ‘‘brane tilings’’. For that reason we first explain the tilings in Section 2.3 before going on to the details of the algorithm.

2.2.2. $\mathcal{N} = 2$ quiver Chern-Simons theory in 2+1

Even before proceeding to brane tilings, let us see how the story with the quiver gauge theories applies to M2 branes. As it was recently discovered, the world volume theory on a stack of M2 branes probing a Calabi-Yau singularity Y_8 can be described by a $(2 + 1)$ -dimensional $\mathcal{N} = 2$ Chern-Simons theory. We can again pick a gauge group for the theory and specify the matter multiplets with their representations. It turns out that we can take the same quiver and superpotential as discussed in the previous section and interpret it as specifying the $(2 + 1)$ $\mathcal{N} = 2$ Chern-Simons Lagrangian. That is, we again have a group $g = U(N)^G$, vector multiplets V_i , bifundamental (or adjoint) chiral multiplets X_{ij} , and a superpotential W , all subject to anomaly cancellation and toric

conditions. The Lagrangian now looks like [9]:

$$\mathcal{L}_3 = \text{Tr} \left(- \int d^4\theta \sum_{X_{ij}} X_{ij}^\dagger e^{-V_i} X_{ij} e^{V_j} - i \sum_i k_i \int_0^1 dt V_i \bar{D}^\alpha (e^{tV_i} D_\alpha e^{-tV_i}) + \int d^2\theta W(X_{ij}) + \text{c.c.} \right). \quad (2.13)$$

There is one extra ingredient here besides the quiver and W to specify the model: the integer-valued parameters k_i for each group factor, called the Chern-Simons levels. They are subject to a constraint

$$\sum_i k_i = 0, \quad (2.14)$$

but are otherwise arbitrary, except they shouldn't be all zero.

Even though the Chern-Simons Lagrangian is quite different from the usual gauge Lagrangian in 4 spacetime dimensions (it does not have kinetic terms!), the calculation of the moduli space is very similar. We again have the F-terms and D-terms that in the case of a single M2 brane probe ($N = 1$) look like:

$$\frac{\partial W}{\partial X_A} = 0, \quad (2.15)$$

$$\sum_A Q_i^A |X_A|^2 = 4k_i \sigma, \quad (2.16)$$

where σ is an auxiliary field. So from the point of view of the moduli space calculation the only difference between D3 and M2 models is that the CS levels k_i introduce a non-zero right-hand side in the D-term equation. A slightly modified version of the ‘‘Forward Algorithm’’ can be performed in a complete analogy to the D3 case to arrive at the toric description of the Calabi-Yau moduli space. Actually, the CS levels introduced in the D-term equation have an effect on the algorithm that the resulting toric variety has one more complex dimension compared to the $k_i = 0$ case. So if a given quiver gauge theory on D3 had a Y_6 moduli space, the M2 counterpart is a Y_8 , an 8-real-dimensional Calabi-Yau moduli space, which is exactly what we want!

More problems with finding consistent M2 world-volume theories arise when checking other requirements of duality besides the moduli space, such as the flow to a SCFT in the IR. With D3 theories the correspondence by now is quite well understood and it is known that it is the ‘‘brane tilings’’ that give the consistent dual theories. In addition there are further restrictions explained in Section 2.4.3 that pick out ‘‘consistent brane tilings’’, which give the fully

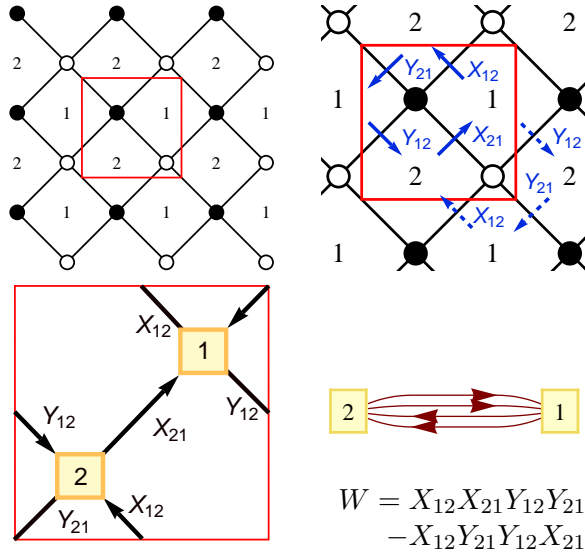


Figure 2.2.: Example of a tiling, periodic quiver and quiver/superpotential.

consistent dual CFTs to $AdS_5 \times X_5$ geometries. Unfortunately such consistency conditions are not yet fully understood for M2 world-volume theories dual to $AdS_4 \times X_7$. However, there is good evidence that the interesting 2+1 dimensional SCFTs are again found among those described by brane tilings.

2.3. Brane Tilings

“Brane tilings” (or “tilings” for short) are objects that give a convenient description of a quiver gauge theory by encoding both the quiver and the superpotential. It is important to stress that not every quiver theory can be described by a tiling. If it can, then we say that a quiver “admits a tiling description”. On the other hand, every tiling can be translated into a quiver and a superpotential. As already mentioned, it is exactly the theories that admit a tiling description that are of interest.

We can define a tiling as an *unoriented bipartite planar graph on a torus*. See Figure 2.2 for one of the simplest examples. Let us explain what this definition actually means. First, a bipartite graph, also known as 2-colorable graph, means that we can assign two different “colors” to the nodes in such a way that edges in the graph always connect nodes of different colors. We conventionally use white and black nodes to indicate bipartiteness. Second, we want the graph to be planar on a two-dimensional torus T^2 . What that means is that it should be possible to draw the graph on a T^2 in such a way that no two edges intersect. We can look at this requirement from a different perspective by

“unwrapping” the torus into a two-dimensional periodic grid. Instead of being planar on a torus, the graph then has to be simply planar and periodic in two dimensions. This representation can be seen in Figure 2.2, and this is where the name “tiling” comes from, since the graph, being planar, then just represents a way to cover the plane in tiles with a bi-periodic pattern. It should still be kept in mind that what this really represents is a graph with *finite* number of edges and nodes, which are contained in the fundamental domain of the pattern. We indicate the fundamental domain in the tiling pictures in red, and the torus can be reconstructed by identifying the opposite edges. For many more examples of tilings the reader is referred to Appendix A.

Now that we have tilings defined as a particular class of graphs, we can go on and explain how these graphs can be interpreted as defining quiver gauge theories. The rules are the following:

- **Faces** in the tiling correspond to gauge group factors, thus the **nodes** in the quiver.
- **Edges** in the tiling correspond to the matter fields, thus **edges** in the quiver. A field is charged under the two groups represented by the adjacent faces, and the direction of the field arrow can be defined to be such, that the white node is on the right side of the arrow.
- The **nodes** in the tilings correspond to the **superpotential terms** in the quiver theory. A term is a product of the fields connected to the node, multiplied clockwise around white nodes and counter-clockwise around black nodes. The sign of the term is determined by the color of the node, we choose white for positive terms and black for negative.

The rules are illustrated also in Figure 2.2. The crucial part is that the tiling encodes the whole theory, that is *both* the quiver and the superpotential, in a single geometrical structure.

Note that these rules can be seen as a kind of *dualization*, which can be performed on any planar graph without a boundary. Since planar graphs have clearly defined faces, one can always interchange faces and nodes, mapping edges to “perpendicular” edges. By performing this operation on the tiling, one gets the quiver on a torus or a *periodic quiver* (also shown in Figure 2.2). This is exactly the quiver of the gauge theory as an abstract graph defined by the previous rules, but if it is kept on a torus as a planar graph, then there is extra information encoded by the faces in the quiver graph: they are precisely the terms in the superpotential. So alternatively we could look at the tiling as a graph dual to the quiver, after the quiver is drawn on a T^2 in such a way that it

is planar and faces represent the superpotential terms. We use this observation when we discuss the classification algorithm in Section 3.4.4.

Let us further discuss the properties that the theories defined by the tilings have, and why they appear to be good candidates for the AdS/CFT duality. First, we can see how the anomaly cancellation condition and the toric condition, which we defined on the quiver gauge theories as additional constraints, arise naturally in the tiling picture. For the anomaly cancellation, consider a face in the tiling, which represents a group node in the quiver. Because of the bipartite nature of the tiling, the nodes alternate between black and white around the face. Because the orientation of the field associated with an edge is defined with respect to the node color, the direction of the field arrows also alternates around the face. As a consequence of that, for each node in the quiver there is always the same number of incoming and outgoing fields. Next, the toric condition is obvious from the tiling. Each edge representing a field stretches between a white and a black node, therefore, it appears twice in the superpotential: once in a positive and once in a negative term.

There is a further restriction on the quiver gauge theories that represent CFT duals to $AdS_5 \times X_5$, imposed by the requirement of superconformality in IR, which turns out to be automatically satisfied by tilings as well. The superconformality condition states that for all groups g_i the following is true [4]:

$$\sum_{X \in g_i} (1 - R_X) = 2, \quad (2.17)$$

where R_X is the R-charge of the field, and the sum is over all fields charged under group g_i (fundamental or anti-fundamental). There is also a requirement that the total R-charge of the superpotential is 2, which means that for each term W_i

$$\sum_{X \in W_i} R_X = 2. \quad (2.18)$$

Even without knowing R-charges of the individual fields, we can derive an identity by relating the total charge of all fields $\sum R_X$. Let us note the number of group nodes by G , the number of fields by E and the number of superpotential terms by N_T . Then by summing (2.17) over all groups we get:

$$\sum_i \sum_{X \in g_i} (1 - R_X) = 2 \sum_X (1 - R_X) = 2E - 2 \sum_X R_X = 2G, \quad (2.19)$$

where the first equality holds because the first sum includes each field twice.

Summing (2.18) over all superpotential terms gives

$$\sum_i \sum_{X \in W_i} R_X = 2 \sum_X R_X = 2N_T, \quad (2.20)$$

since the first sum again includes every field twice. Now equating $\sum_X R_X$ from (2.19) and (2.20) we get

$$E - G = N_T, \quad (2.21)$$

which is a constraint on the quiver gauge theory, relating the number of fields, groups and superpotential terms. The remarkable fact is that this condition, which arises non-trivially from the superconformality, is satisfied for all tiling theories! The reason is that (2.21) from the tiling picture represents the *Euler relationship* between the number of nodes, edges and faces in a simplex, and it is always satisfied as long as the simplex has no boundary and is on a T^2 .

To summarize once again, the brane tilings give us a class of quiver gauge theories that automatically satisfy several requirements imposed on a dual CFT living on D3 branes probing a Calabi-Yau toric singularity. Given a tiling, it is still not *guaranteed* to give a consistent dual CFT, as we see in Section 2.4.3, but there is a good chance that it does. Regarding M2 world-volume theories, the consistency conditions are not as clear, but we are also led to believe that tilings provide a wide class of consistent $AdS_4 \times X_7$ duals.

Finally, to finish an argument on why the brane tilings are thought to provide a good picture of duals, we have to mention the NS5-D5 brane construction (see [5] for an extended review). It turns out that a stack of D3 branes at a toric Y_6 singularity can be shown to be T-dual to a certain system of NS5 branes and D5 branes. From a particular 2-dimensional projection the system looks like a T^2 torus, with NS5 branes creating a grid of intersecting lines and D5 branes stretching in the holes between them. This, in fact, provides the *physical* interpretation of the tiling: the edges represent the NS5 branes and faces represent the D5 branes. This interpretation is the reason why these objects are called *brane* tilings. It can be shown that in the IR limit the NS5-D5 system will be described by a quiver gauge theory with fields living on the edges of the tilings, arising from strings stretching between D5 branes across NS5, and interacting at the intersections of NS5. This view provides the most complete physical picture of the $(AdS_5 \times X_5) / (\mathcal{N} = 1$ quiver gauge theory) duality: gravity on $AdS_5 \times X_5$ is dual to a world-volume theory on a stack of D3 branes at a Y_6 singularity, which is in turn dual to a NS5-D5 brane system, which in the low-energy limit is described by a quiver gauge theory given by a tiling.

2.4. Moduli space calculations

The last ingredient we need for the classification algorithm is the calculation of moduli spaces in order to establish the duality between tilings and toric Calabi-Yau manifolds. The Calabi-Yaus are represented using the language of toric geometry, which we briefly mention first. For a full introduction to toric varieties see [31]. Then we describe the “Forward Algorithm” which we use in this work to calculate moduli spaces. We see that in the process there might be a couple of obstacles further preventing a tiling to give a consistent dual CFT.

2.4.1. Toric geometry

In this work we are dealing with a class of X_5 or X_7 Sasaki-Einstein background manifolds, giving rise to *toric* Calabi-Yau cones Y_6 or Y_8 . We view them here as complex 3-fold CY_3 and 4-fold CY_4 respectively. One of the main reasons to restrict ourselves to these backgrounds is that the toric Calabi-Yau spaces can be described and classified in complete generality by using the so-called *toric diagrams*. Then the properties of the spaces can be analyzed even without the knowledge of the explicit metric. Also, as we see in the next section, the moduli space of a toric quiver gauge theory can be calculated explicitly in precisely the form of the toric diagram.

In general, a toric diagram is a set of points on an integer lattice \mathbb{Z}^n . It defines a *toric variety*, which is an n -dimensional complex space. We don’t really explain how the variety is defined, for that see [31], or a quick review in [4]. For examples of diagrams with varieties that they represent see Appendix A.

The toric CY_3 and CY_4 of interest can be described by \mathbb{Z}^3 or \mathbb{Z}^4 toric diagrams respectively. It is convenient to represent the points on a lattice as a matrix, containing the set of integer vectors as columns. For example

$$G_t = \begin{pmatrix} 0 & 1 & 1 & 2 & 1 \\ 0 & 0 & 0 & 0 & 1 \\ 1 & 1 & 1 & 1 & 1 \end{pmatrix}, \quad (2.22)$$

where each column indicates a point on \mathbb{Z}^3 . There are a few extra important properties of toric diagrams that we need. First, the diagram is defined only up to $GL(n, \mathbb{Z})$ transformation of the coordinates on the lattice. From the point of view of the representative matrix G_t , we can multiply it on the right:

$$G_t \rightarrow U \cdot G_t \quad (2.23)$$

by any integer matrix U of determinant one. From the point of view of the diagram picture, rotation and “skew” transformations can be applied, without changing the meaning of the diagram, i.e. it still represents the same toric variety.

Another important property concerns Calabi-Yau toric varieties: it turns out their toric diagrams can always be transformed in such a way, that one row in G_t matrix contains all 1, as in (2.22). So for the purpose of graphical representation we can always drop one row, so that a CY_3 is represented by a \mathbb{Z}^2 diagram and CY_4 is represented by a \mathbb{Z}^3 diagram. It is these 2-dimensional diagrams representing CY_3 (or Y_6) moduli spaces that are listed in the Appendix A. For example G_t in (2.22) is graphically displayed as Figure 2.3 and represents a $\mathbb{C}^2/\mathbb{Z}_2 \times \mathbb{C}$, which is the moduli space of the model labelled (2.1).

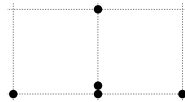


Figure 2.3.: Example of a toric diagram for $\mathbb{C}^2/\mathbb{Z}_2 \times \mathbb{C}$, which is the moduli space of the (2.1) model.

Finally, let us note that from the point of view of the definition of toric varieties there is no meaning to a lattice point being occupied by more than one diagram point like, for example, the point $(1, 0, 1)$ in (2.22). This “multiplicity”, however, comes out from the moduli space calculation algorithm, and has an importance for the further analysis of the models, therefore, we always keep it visible in the diagrams.

2.4.2. Forward algorithm

Given a tiling, there is a way called Forward Algorithm to solve the F-terms and D-terms and calculate the moduli space as a toric diagram. We don’t provide an explanation here of why exactly it finds the solution, and only cite the results needed for the computation. A detailed discussion can be found in the references, including the reviews [4, 5]. The algorithm works either with pure tiling, defining a D3 world-volume theory, or with tiling plus Chern-Simons levels, which defines an M2 world-volume theory. The resulting moduli space is CY_3 or CY_4 respectively. The algorithm is summarized in the following diagram [11]:

$$\begin{array}{l}
\boxed{\text{INPUT 1:}} \\
\text{Superpotential} \\
\rightarrow P_{E \times c} \rightarrow (Q_F)_{(c-G-2) \times c} = \ker(P) \\
\searrow \\
\boxed{\text{INPUT 2:}} \\
\text{Quiver} \\
\rightarrow d_{G \times E} \rightarrow (Q_D)_{(G-2) \times c} = \ker(C)_{(G-2) \times G} \cdot \tilde{Q}_{G \times c} \\
\text{(where } d_{G \times E} = \tilde{Q}_{G \times c} \cdot (P^t)_{c \times E}\text{)} \\
\nearrow \\
\boxed{\text{INPUT 3:}} \\
\text{CS Levels} \\
\rightarrow C_{2 \times G} \\
\downarrow \\
(Q_t)_{(c-4) \times c} = \begin{pmatrix} (Q_D)_{(G-2) \times c} \\ (Q_F)_{(c-G-2) \times c} \end{pmatrix} \rightarrow \boxed{\text{OUTPUT:}} \\
(G_t)_{4 \times c} = \ker(Q_t)
\end{array} \tag{2.24}$$

This shows the calculation of the CY_4 , given a tiling and Chern-Simons levels, but it can also be used in almost the same way to produce CY_3 . Constants G and E again mean the number of groups and fields in the tilings, and c is the number of so-called *perfect matchings*, which we define below. The algorithm amounts to basically some linear algebra manipulations with the matrices P , d and C in order to produce G_t , the toric diagram of the moduli space variety. All we need to define then are the input matrices.

First, $d_{G \times E}$ is a G -by- E matrix describing the quiver, called the ‘‘incidence matrix’’. Each row corresponds to a group node and each column defines a field, with value $(+1)$ in the row where the field arrow starts and (-1) where the arrow ends, with other entries set to zero. A column corresponding to an adjoint field would have zeros in all rows.

The matrix C contains the values of the Chern-Simons levels in one row, and another row filled by 1:

$$C = \begin{pmatrix} 1 & 1 & 1 \\ k_1 & k_2 & k_3 \end{pmatrix}. \tag{2.25}$$

We can also use this matrix to get a CY_3 moduli space by setting all $k_i = 0$. Then the dimensionalities of the matrices change slightly from those in (2.24), and the output G_t actually becomes a matrix with only 3 rows rather than 4, as needed.

Finally, we need the matrix P which defines the perfect matchings, that are implied by the superpotential. In order to find it we use the algorithm outlined in the Appendix B of [11]. The procedure is as follows. Let us define a matrix K , which is one of the versions of the so-called *Kasteleyn matrix*. Let the rows correspond to the positive terms of the superpotential, and the columns to the negative terms. Then to each entry K_{ij} we assign the sum of the fields that are

included both in the i 'th positive term and the j 'th negative term. Using the earlier example of a superpotential from (2.7):

$$W = \text{Tr}(\Phi_1 X_{12} X_{21} - \Phi_1 X_{13} X_{31} + X_{13} X_{32} X_{23} X_{31} - X_{12} X_{23} X_{32} X_{21}), \quad (2.26)$$

the Kasteleyn matrix would be:

$$K = \begin{pmatrix} \Phi_1 & X_{12} + X_{21} \\ X_{13} + X_{31} & X_{32} + X_{23} \end{pmatrix}. \quad (2.27)$$

Then if we take the determinant of K :

$$\det K = \Phi_1 X_{32} + \Phi_1 X_{23} - X_{12} X_{13} - X_{12} X_{31} - X_{21} X_{13} - X_{21} X_{31}, \quad (2.28)$$

each monomial corresponds to a *perfect matching*. We see that there are 6 of them here, so $c = 6$. The perfect matching matrix $P_{E \times c}$ then just describe which fields are included in which perfect matchings. For each row i corresponding to a field and each column j corresponding to a perfect matching P_{ij} is 1 if the fields corresponds to the perfect matching, and 0 if it doesn't.

2.4.3. Extra consistency conditions

Before finishing with the background discussions let us mention final things that can go wrong with constructing dual CFT from the tiling. First, in order to calculate the moduli space, as described in the previous section, we have to construct the perfect matching matrix P . A geometrical meaning of a perfect matching on a tiling is that it provides a collection of field edges such that each node touches exactly one edge in the collection. Actually, this is why they are called ‘‘perfect matchings’’. All possible ways of picking a subset of edges this way gives the set of c perfect matchings. However, it can happen in some cases that a tiling does not admit a perfect matching altogether. One simple example where that happens is if a tiling has unequal number of black and white nodes (note that it is not forbidden by the toric condition itself). For such tilings the calculation of the moduli space breaks down because $c = 0$, and matrix P is undefined. We immediately discard such tilings as being candidates for consistent CFT theories both in D3 and M2 brane cases, and they do not appear anywhere in this work.

There is another more subtle consistency condition which turns out to be imposed on the world-volume theories of D3 branes. After calculating the 2-dimensional toric diagram of the CY_3 corresponding to a tiling, we can compute the *area* of the convex hull of the diagram. Let us call it A . Note that the area

is invariant under the $GL(2, \mathbb{Z})$ transformations. Now, it turns out that there is a problem with the 4-dimensional CFT *unless*:

$$G = 2A, \tag{2.29}$$

where G is again the number of groups in the theory. The quiver gauge theories for which this is not satisfied encounter further problems in the flow to IR, and do not represent a consistent CFT theories [26, 27, 28]. We refer to these models as *inconsistent tilings*. As can be seen in Appendix A they actually constitute the majority of all the possible tilings. However, it has to be stressed that the inconsistencies in the IR flow are only known to be encountered for the case of dual CFT_4 living on D3 branes and *not* for M2 brane world volume theories. As far as we know, the inconsistent tilings can provide perfectly valid CFT_3 duals.

3. Classification Algorithm

3.1. Motivation

With the background material behind us, let us proceed to the discussion of the results of this work. The main objective of this project is to have a way of *listing the possible brane tilings*. Naturally, the full list is impossible due to being infinite, but we can organize it by increasing value of some complexity parameter. Then we want to be able, in principle, list all the tilings up to a chosen maximum value of such parameter. Before we go on with describing our approach to the problem, let us first review why we think such classification would be useful.

As discussed in Section 2.1 the ultimate interest is to explore the dual CFTs for various $AdS_5 \times X_5$ and $AdS_4 \times X_7$ backgrounds. For the cases where the Calabi-Yau cones CY_3 and CY_4 are toric, we can describe a given background by a two-dimensional or a three-dimensional toric diagram respectively. If we can then find a brane tiling that produces the CY_n as the moduli space and satisfies additional consistency conditions, we have found the dual CFT.

For the case of CFT_4 on D3 branes there is, in fact, a procedure called the “Inverse Algorithm” that does just that: starting with a two-dimensional toric diagram it can construct the corresponding brane tiling directly [3]. It is not as straightforward as the Forward Algorithm and there are some ambiguities involved, but it provides a complete method for finding the toric $AdS_5 \times X_5$ duals.

However, with the recent applications of tilings to toric $AdS_4 \times X_7$ dualities, the story is far from being complete. The toric diagram here is three-dimensional, and unfortunately no analog of universal Inverse Algorithm exists. We do, on the other hand, still have the Forward Algorithm as described in Section 2.4.2. This suggests the following “brute-force” approach to the inverse algorithm: we could systematically enumerate the possible brane tilings, apply the forward algorithm in each case, and gather a catalog of the resulting CY_4 toric diagrams. Then given a background X_7 of interest, we can look up the corresponding tiling, once it is in the catalog. The role of *inconsistent tilings* is important here, since they have not been analyzed in the context of

CFT_4 dualities, and provide a large class of new models.

The enumeration of all possible tilings would also be of some value even in the context of D3 brane theories. Up till now various different backgrounds have been studied individually, including some infinite families of CY_3 spaces, however, there is still no systematic classification of the possibilities from the brane tiling perspective. In this work by scanning through the tilings systematically it would be interesting to see if there are any models that have been missed so far by the individual studies.

Finally, bipartite periodic graphs appear in various other fields in physics and mathematics, so the classification of such graphs might be of some interest by itself.

3.2. Method Overview

Here we present a method to systematically enumerate the brane tilings. Given the combinatoric complexity of the problem, we choose a purely computational approach and present a clearly defined algorithm that could, in principle, list all the tilings in increasing complexity.

The total number of tilings is, of course, infinite, so the first thing we must do is choose some parameters to help organize the classification. The natural parameters of a tiling are the number of nodes in the fundamental domain of the tiling N_T and the number of tiles G . The number of edges in the fundamental domain E is then fixed by the Euler condition:

$$E = G + N_T. \tag{3.1}$$

From the quiver gauge theory perspective these numbers are the number of nodes in the quiver G , the number of fields E and the number of terms in the superpotential N_T .

Unfortunately working directly with tilings is computationally quite difficult. As the main objects of a tiling are geometrical, it is not obvious how to set up a systematic calculation of the possible periodic tilings with some parameters (N_T, G) , especially without making any a priori assumptions about the shapes of the tiles. For that reason we choose *quiver gauge theories* as our main working objects [11]. The method we choose is to enumerate all possible quivers and superpotentials, and then check which ones admit a tiling description. As each brane tiling corresponds to a quiver gauge theory, we can be sure that every tiling will be generated.

In summary, we propose the following algorithm for the classification of

tilings:

1. Fix the order parameters (N_T, G) .
2. Enumerate all distinct *irreducible* quivers with G nodes and $E = G + N_T$ fields.
3. For each quiver enumerate all possible superpotential terms satisfying the toric condition. This gives the full list of possible quiver gauge theories for (N_T, G) .
4. Try to reconstruct the tiling for each quiver gauge theory. If we succeed, we add it to the classification, otherwise we conclude that the gauge theory doesn't have a tiling description.

Each step here requires further explanation. But let us postpone this and introduce the concept of doubling, which will provide some important insights and an understanding of the term irreducible quiver. This will help us to simplify the task of classification considerably.

3.3. The Doubling Process and Quadratic-Node Tilings

Let us consider an operation on a quiver where we replace an edge with two edges, both connected to a node of valence 2. We shall call this process “doubling”. Doubling defines a new theory when applied to any of the fields in a quiver. From the perspective of the tiling this operation replaces an edge by two edges and a face surrounded by only these 2 edges (see Figure 3.1). This is known as a double bond [10] [30]. It is important to note that the doubling procedure keeps the number of terms in the superpotential N_T constant, because it increases both G and E by one.

By repeatedly applying doubling to the fields in a given model we can produce infinitely many descendent theories. For example, starting with a simple \mathbb{C}^3 model we can arrive at the whole class of models, where there is a central node with three outgoing loops, each containing some number of extra nodes [11] (see Figure 3.2). In the tiling picture this simply corresponds to the one and the same one-hexagon tiling, but with each of the three field edges replaced by a multi-bond containing arbitrary number of edges running in parallel between the two nodes.

The important observation is that this doubling process is always reversible. If we are given a brane tiling with double-(or multi-)bonds, we can always

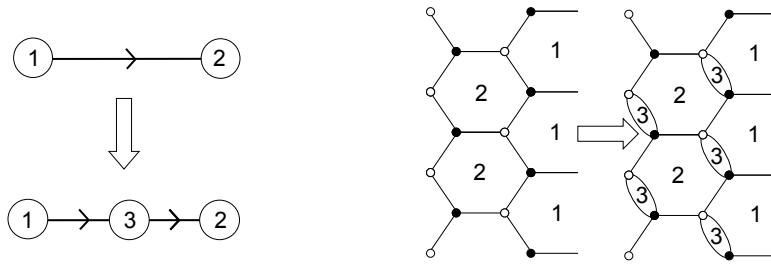


Figure 3.1.: The Action of the Doubling Process on (i) the Quiver and (ii) the Tiling.

remove them by the process of “higgsing”. From the quiver perspective, we can remove all nodes of valence 2 from the quiver (Figure 3.3). Let us call quivers with at least one node of valence two “reducible”. If a quiver isn’t reducible it is said to be “irreducible”.

Given that we understand the action of the doubling process on both the tiling and the quiver, we may consider from now on only irreducible quivers (or tilings with no double-(or multi-)bonds). All reducible quivers can easily be generated by applying the doubling process to the set of irreducible quivers. This is a crucial observation, because it lets us effectively ignore an infinite “direction” in the space of tilings, thus allowing us to concentrate on the much smaller class of brane tilings, which are not related by this simple transformation.

We have to note, however, that there is one caveat in this argument. For some reducible quivers the higgsing procedure results in a brane tiling, which has nodes connected only by two edges (valency 2 nodes), as seen in Figure 3.4. This means that the corresponding quiver gauge theory has a superpotential with quadratic terms in it. We call such models quadratic-node tilings.

The quadratic-node tilings are perfectly valid according to our definition of tilings in Section 2.3, however, they are not normally considered in the context of quiver gauge theories on D3 or M2 branes. This is because the quadratic superpotential terms indicate massive fields, which become non-dynamical in the infrared limit [3]. Since we are interested in analyzing the IR limit of these gauge theories, the massive fields should be integrated out using their equations of motion. The corresponding effect on the tiling is that the quadratic node can be removed, gluing the two adjacent nodes together (see Figure 3.5).

For this reason we exclude the tilings with quadratic nodes from our classification. However, this means that the models where quadratic nodes are only absent because of multi-edges (such as the one in Figure 3.4) can not be re-

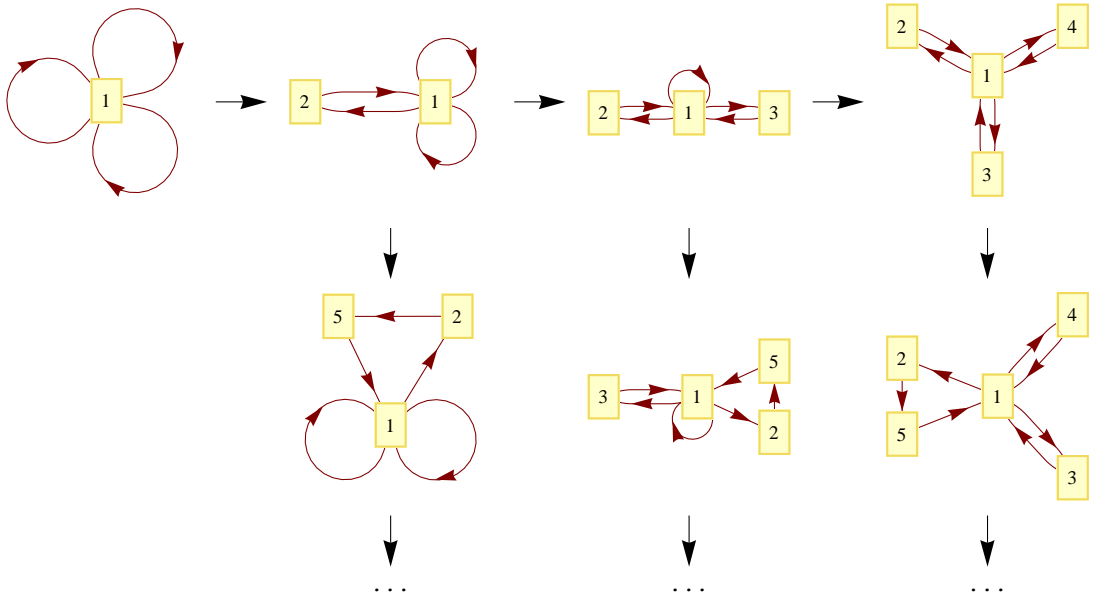


Figure 3.2.: Quivers generated by applying doubling to \mathbb{C}^3 .

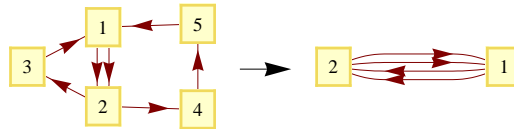


Figure 3.3.: Reduction of a quiver by removal of single-in, single-out nodes.

covered from the irreducible quivers simply by the doubling procedure. To get back such tilings from the classification in this paper we would have to combine the doubling procedure together with an insertion of two extra nodes.

With the procedure of doubling in mind, we restrict our attention to the classification of brane tilings without multi-edges and without quadratic nodes. Let us now go over the steps in the classification algorithm in more detail.

3.4. Algorithm in detail

3.4.1. Order parameters

Let us recall the two parameters we are going to use to order our classification - (N_T, G) . Constraints on the tilings discussed in the previous section allow us to put limits on the possible values of G for each value of N_T .

Firstly, let us consider the requirement that the quiver is irreducible. This is

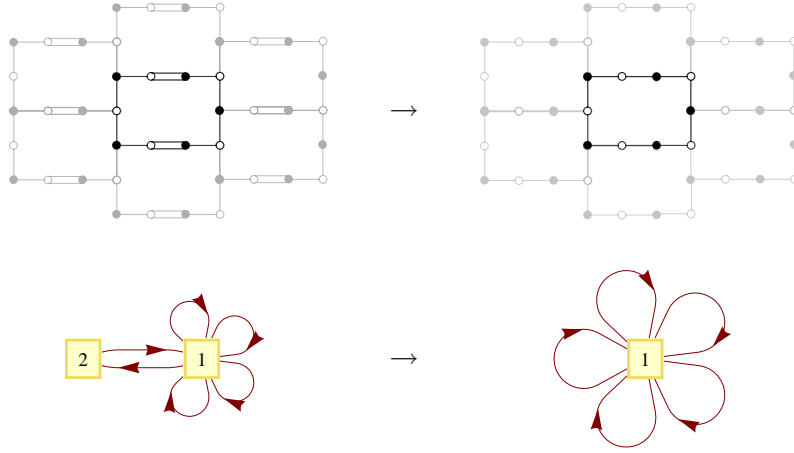


Figure 3.4.: Reduction of a quiver resulting in quadratic-node tiling.

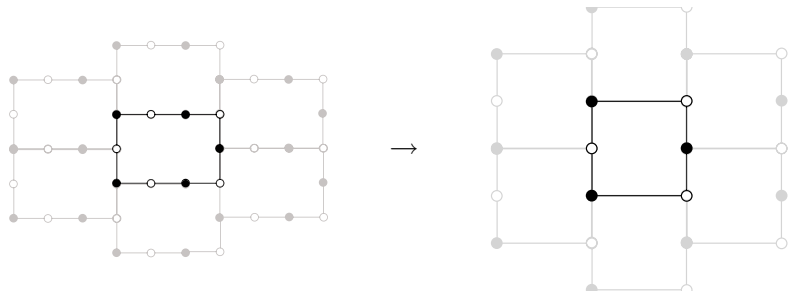


Figure 3.5.: Reduction of a quadratic-node tiling.

equivalent to saying that there should be no nodes in the quiver of valency 2. As the nodes must have the same number of incoming and outgoing edges, each node should be of valency 4 or higher. We also have the following relationship for any quiver:

$$E = \frac{1}{2} \sum_{i=1}^G n_i, \quad (3.2)$$

where n_i is the order of node i . We can therefore conclude that we need a minimum of

$$E_{min} = 2G \quad (3.3)$$

fields for irreducible quivers. Using $E = G + N_T$ we have

$$(N_T)_{min} = G \quad (3.4)$$

N_T	G_{min}	G_{max}	E_{min}	E_{max}
2	1	2	3	4
4	2	4	6	8
6	3	6	9	12

Table 3.1.: Values of order parameters explored.

for fixed G or, for fixed order parameter N_T , we have a maximum value of

$$G_{max} = N_T \tag{3.5}$$

for order parameter G , if we only consider irreducible quivers. Most importantly, this tells us that for given N_T there is a finite number of models with irreducible quivers. This statement is clear from the brane tiling perspective. If the number of nodes in a tiling is fixed, there are only a finite number of edges that can be added to the tiling before producing multi-bonds.

A lower bound for G for fixed N_T can also be found. As the tilings are irreducible, this means the minimum valency of all nodes is 3. Let us use (3.2) on the tiling, counting only edges and nodes in the fundamental domain. Now the edges are again fields and the nodes are the superpotential terms, giving us the bound:

$$E_{min} = \frac{3}{2}N_T. \tag{3.6}$$

Using $E = G + N_T$ we get

$$G_{min} = \frac{1}{2}N_T, \tag{3.7}$$

which is our lower bound on the parameter G for given N_T , and so we have for fixed N_T

$$\frac{1}{2}N_T \leq G \leq N_T \tag{3.8}$$

It is now clear how to organize the classification. We consider each N_T in an increasing order, exploring the possible G values at each step. The number of possible superpotential terms N_T is, of course, still unbounded, and we are limited only by our technical abilities and curiosity. In this paper we explore the models up to *six* terms in the superpotential. The summary of order parameters considered is given in Table 3.1.

3.4.2. Finding Quivers

Once we fix the parameters (N_T, G) , the next step is to enumerate all of the possible quiver graphs with a given number of nodes G and edges E . The task

is quite straightforward, but it has to be handled with a little care, to avoid the algorithm becoming too computationally expensive as G and E grow larger.

A naive approach would be to consider all possible ways of connecting G nodes with E edges. With $G(G-1)$ ways of drawing a directed edge, we would have the order of

$$(G(G-1))^E \tag{3.9}$$

possible graphs to consider, which is clearly too large for, say, $G = 6, E = 12$. However, we are only interested in a very small fraction of these graphs, satisfying the anomaly cancellation condition, requiring that nodes have the same number of incoming as they do outgoing edges. Only such quivers can admit a tiling description

The key idea of this efficient algorithm for finding all possible quivers is to incorporate this condition into the construction of the quiver. We achieve this by making the following observation: a graph has the same number of incoming and outgoing edges at each node if and only if it can be decomposed into a sum of cycles. By “sum” we mean that we take the union of nodes and the union of edges from the constituent cycles, while keeping the labels of the nodes intact (so that $1 \rightarrow 2 \rightarrow 3 \rightarrow 1$ is different from $1 \rightarrow 2 \rightarrow 4 \rightarrow 1$). An example of such a decomposition is shown in Figure 3.6.

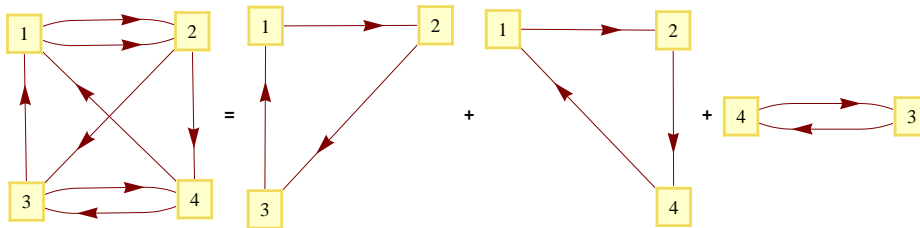


Figure 3.6.: Decomposition of a graph into cycles.

In order to build a complete list of quivers for a given G and E , we must first consider all of the possible cycles over G nodes. Then we take combinations of those cycles such that the total number of fields adds up to E . This way we have all of the quivers that satisfy the anomaly cancellation condition. This approach is significantly faster than the naive method, and is efficient enough to easily produce all of the quivers found in this paper using a modern computer.

3.4.3. Finding Superpotentials

After finding the quivers, we must construct all possible quiver gauge theories. This is done by finding all of the superpotentials W that could be associated

with each quiver.

As explained in Section 2.2 we know that gauge invariant terms correspond to *cycles* in the quiver. The first step of the algorithm is then to find all gauge invariant term candidates by finding all cycles of the quiver graph. The cycles are allowed to include each field at most once, and also they should be of length 3 or more, because we don't consider quadratic terms.

Next, we try to combine the possible terms into full superpotentials, satisfying the necessary rules. That is, we require the toric condition, that each field appears once in a positive and once in a negative term. We also fix the overall number of positive and negative terms to be the same, in order for the resulting tiling to admit perfect matchings.

By considering all combinations subject to these constraints we arrive at a set of quiver gauge theories that can be defined on a given quiver. However only a small fraction of these models can actually admit a tiling description, and for that we need the final step in the algorithm.

3.4.4. Reconstructing Tilings

The final step in the algorithm is to check for whether a given quiver gauge theory can correspond to a brane tiling and then to find this tiling.

The way we proceed is by using an object called a periodic quiver [3]. It is the graph dual of the tiling, where nodes are groups, fields are edges and faces are superpotential terms. Since the data generated so far comprises of a list of quivers and superpotentials, the task of finding the tilings reduces to whether we can unfold the quivers into bi-periodic graphs of the plane. If we can find a periodic quiver from an ordinary quiver and a superpotential, then we know that the model admits a tiling description, and we can easily find its dual graph, the brane tiling.

The algorithm used to produce the tilings is as follows. We are given the quiver Q and superpotential W . The idea is that we try to build up the fundamental domain of the periodic quiver. To do that, firstly, we represent each term in W by a polygon with edges around its perimeter representing fields. We choose the fields have a clockwise orientation for positive terms and a counter-clockwise orientation for negative terms. These polygons will be the faces of the periodic quiver.

Next, we fit these polygons together into one shape by gluing edges that represent the same field together. The process is always possible due to the toric condition on the superpotential. The shape generated is our candidate for the fundamental domain. The test this shape must pass is whether we can

identify opposite edges in a way such that the shape forms a 2-torus. If we can do this we have found a periodic quiver and so a brane tiling.

Let us illustrate this procedure with an example known as the suspended pinch point [3]. The quiver is shown in Figure 3.7 and the superpotential is the following:

$$W = \phi_1 \cdot X_{12} \cdot X_{21} - \phi_1 \cdot X_{13} \cdot X_{31} - X_{12} \cdot X_{23} \cdot X_{32} \cdot X_{21} + X_{13} \cdot X_{32} \cdot X_{23} \cdot X_{31} \quad (3.10)$$

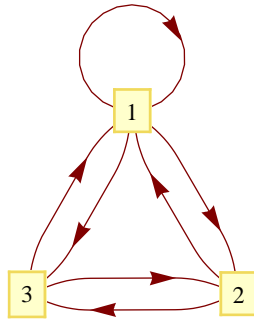


Figure 3.7.: *SPP* quiver.

There are four terms in the superpotential, which we represent by four polygons - two “triangles” corresponding to the cubic terms and two “squares” corresponding to the quartic terms (Figure 3.8). Recall that the arrows around the faces go clockwise for positive and counter-clockwise for negative terms. We can now treat the problem just like a jigsaw puzzle: we have to put these pieces together allowing only edges corresponding to the same field to touch. If it is possible to fit these pieces together to form a 2-torus, it means we have a periodic quiver.

Let us consider the SPP model and glue the four terms together into one shape, by identifying the three fields X_{21} , ϕ_1 and X_{13} . This shape is our candidate for the fundamental domain. It is unimportant as to which three fields we pick to glue together; a different choice just results in generating a different fundamental domain of the periodic quiver. Next we attempt to deform the shape into a rectangle that can be used to tile the plane. If this is possible we have found the model’s periodic quiver¹.

¹In some more complicated cases, it is possible to generate a shape that has a pair of identical fields adjacent to each other. We simply glue together all of these repeating edges, until we have a shape with no such repeated edges. We then test whether this shape can be used to tile the plane.

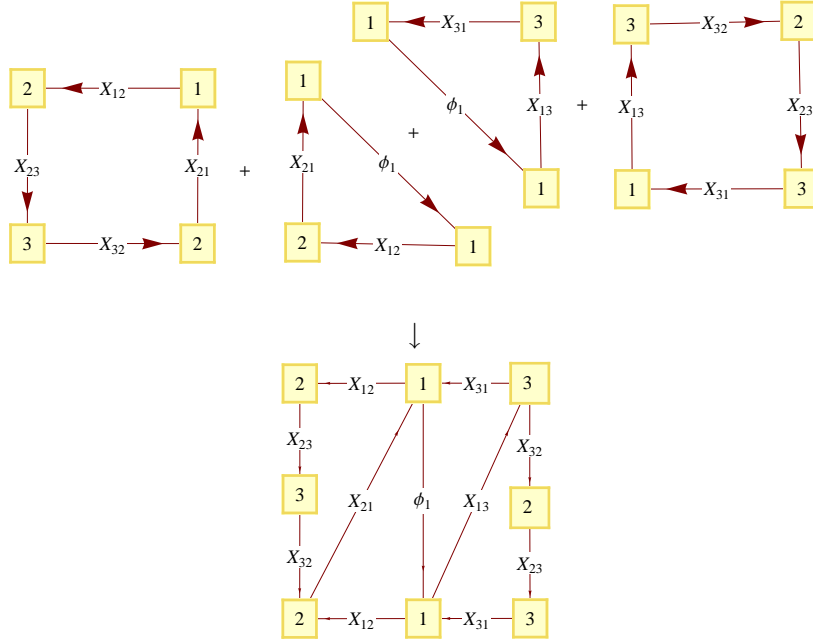


Figure 3.8.: Combining the superpotential terms into a fundamental domain of the periodic quiver.

We can see in Figure 3.8 that it is possible to find a periodic quiver for the SPP. By glancing at the rectangle, we can see that it is possible to use it to tile the plane with only edges corresponding to identical fields touching. We can equivalently see that the shape generated is really a 2-torus. The top and bottom sides of the rectangle can be identified directly along (X_{12}, X_{31}) , effectively turning the rectangle into a cylinder. Then the ends of the cylinder each consist of (X_{32}, X_{23}) , and even though they are not exactly the same on the rectangle, the cylinder can be “twisted” so that the ends are correctly identified.

A key part of the algorithm is this check for whether the resulting fundamental domain can be wrapped to make a torus. A given quiver gauge theory admits a tiling description if and only if that is possible. A simple shape that fails this check is one that has fields $(\phi_1, \phi_1, \phi_2, \phi_2)$ forming the perimeter of a rectangle.

If the construction of a periodic quiver works, we can easily extract the brane tiling from it by finding the dual graph. Firstly, we draw the periodic quiver with our “fundamental rectangle”. Then we insert a white or black node at the center of each face according to whether the arrows go clockwise or counter-clockwise around the perimeter of the face. By replacing edges as in Figure 3.9 we build the dual graph (the brane tiling). In the case of the SPP, we see that

the tiling consists of two hexagons with one of them divided by a diagonal.

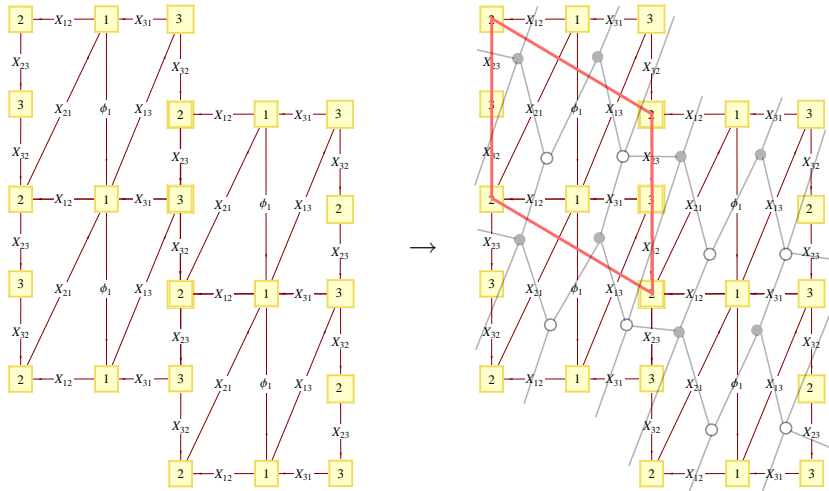


Figure 3.9.: From periodic quiver to brane tiling for *SPP*.

The reader should note that while the algorithm generates a complete list of tilings, it fails to produce aesthetically pleasing pictures. In order to display the tiling in terms of regular geometrical shapes, such as hexagons, squares or octagons we must either find the pattern by inspection, or to rely on other algorithms that display planar periodic graphs neatly. In fact, such an algorithm to nicely render a planar periodic graph was also developed during this project, and it was used to automatically produce the tiling pictures shown in Section 4 and Appendix A.

4. Result Overview

We have used a *Mathematica* implementation of the algorithm described in this paper to generate all irreducible tilings that have at most 6 superpotential terms. The computation only took a couple of hours on an ordinary desktop computer. We believe the computation can be further optimized to be an order of magnitude faster. A full list of all of the tilings generated is given in Appendix A. To be precise, the algorithm produced all distinct unoriented graphs with the following properties:

- Bipartite (or 2-colorable).
- Planar on T^2 or equivalently planar bi-periodic.
- No faces with only 2 bounding edges (meaning no multi-bonds).
- All nodes have valency of at least 3 (meaning no quadratic terms).
- Graph admits a *perfect matching*, i.e. subset of edges such that each node is covered exactly once.
- Limited to maximum 6 nodes.

In this section we briefly discuss the models found.

We start by considering the case of just two terms in the superpotential. Here we only have a choice of one or two gauge groups, and we find one possible tiling for each case. These are the most familiar models: the \mathbb{C}^3 with the one-hexagon tiling and the conifold \mathcal{C} with the two-square tiling (see Figure 4.1). Both of them are consistent tilings [2]. Also the conifold tiling has proved useful in studying the ABJM theory on M2 branes [10].

Let us now consider the 6 tilings generated with with four superpotential terms. With the minimal possibility of two gauge groups and six fields we find the two-hexagon model, or $\mathbb{C}^2/\mathbb{Z}_2 \times \mathbb{C}$ [2]. Among the models with three and four groups we have the *SPP*, Phase I of \mathbb{F}_0 and Phase I of L^{222} (Figure 4.2). We also find the two models labeled as (2.3) and (2.6), which are inconsistent in 3+1 dimensions (Appendix A).

Another elegant way of generating all of the models with four superpotential terms comes from considering the hexagon as the fundamental unit of a tiling.

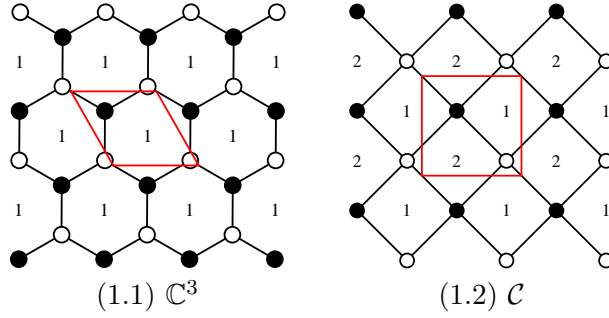


Figure 4.1.: Consistent tilings with two superpotential terms.

Let us start with the two-hexagon tiling. Adding new edges to a tiling keeps the number of superpotential terms the same but increases the number of gauge groups. We can find all tilings with 4 superpotential terms by adding edges across faces of the two-hexagon model. We find that there are two inequivalent ways of adding one diagonal to one of the hexagons, which give the models with three gauge groups (2.2) and (2.3) (see Appendix A). If we add a second diagonal to the tilings we find the remaining three tilings with four gauge groups. This procedure of finding the tilings by adding diagonals also works for the case with two superpotential terms. We start with the basic one-hexagon tiling and find the conifold model by adding one diagonal.

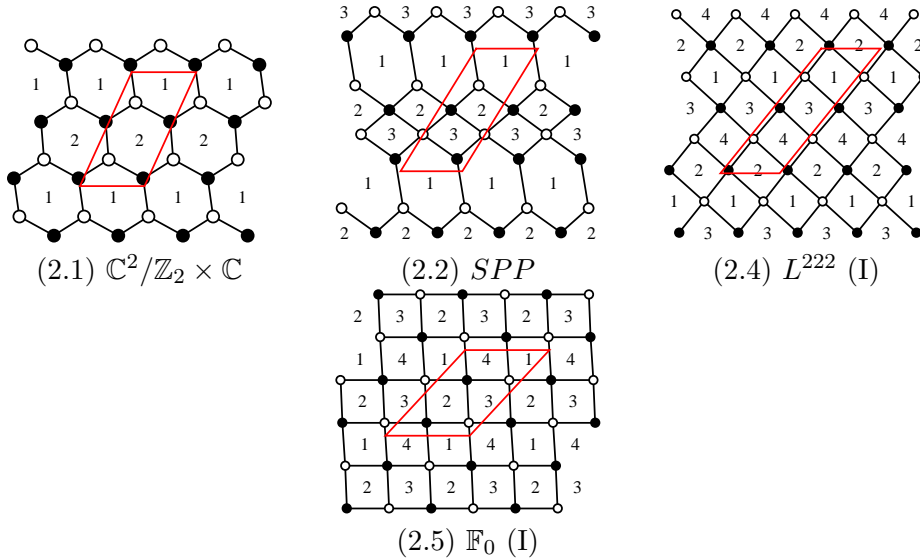


Figure 4.2.: Consistent tilings with four superpotential terms.

Let us now consider the models with six terms in the superpotential. Our algorithm generates a total of 37 different tilings, each having three to six gauge

groups. Of these tilings, only 10 models give rise to consistent tilings. We find that all of the consistent tilings are either phases of L^{aba} or $Y^{p,q}$ families, or one of the del-Pezzo surfaces. Specifically, we find the models dP_0 (or $\mathbb{C}^3/\mathbb{Z}_3$), dP_1 , dP_2 , dP_3 , L^{030} (or $\mathbb{C}^2/\mathbb{Z}_3 \times \mathbb{C}$), L^{131} , another phase of L^{222} , L^{232} , L^{333} and $Y^{3,0}$ (see Figure 4.3). The other models are not as familiar, because they fail the usual 3+1 dimensional consistency condition.

We may wish to gain further insight by considering the procedure of adding diagonals to a 3 hexagon tiling, as we did for the 2 hexagon tiling. Unfortunately we are unable to generate all tilings with 6 superpotential terms using this method as there is a model that has an octagon. However, we may achieve the result if we start with some larger “base figure” than a hexagon. We can consider a model with six superpotential terms, but only *one* gauge group in the quiver and seven adjoint fields. Such a model would inevitably have quadratic terms in the superpotential, and so is not included in this classification.

By considering all possible base figures and by adding diagonals to these base figures in all possible ways, it should be possible to generate all of the tilings in this paper in a matter of minutes rather than hours as this is a computationally a lot easier. This idea is a possible direction for further work as it could help us to find more complex tilings without the need for greater computational power.

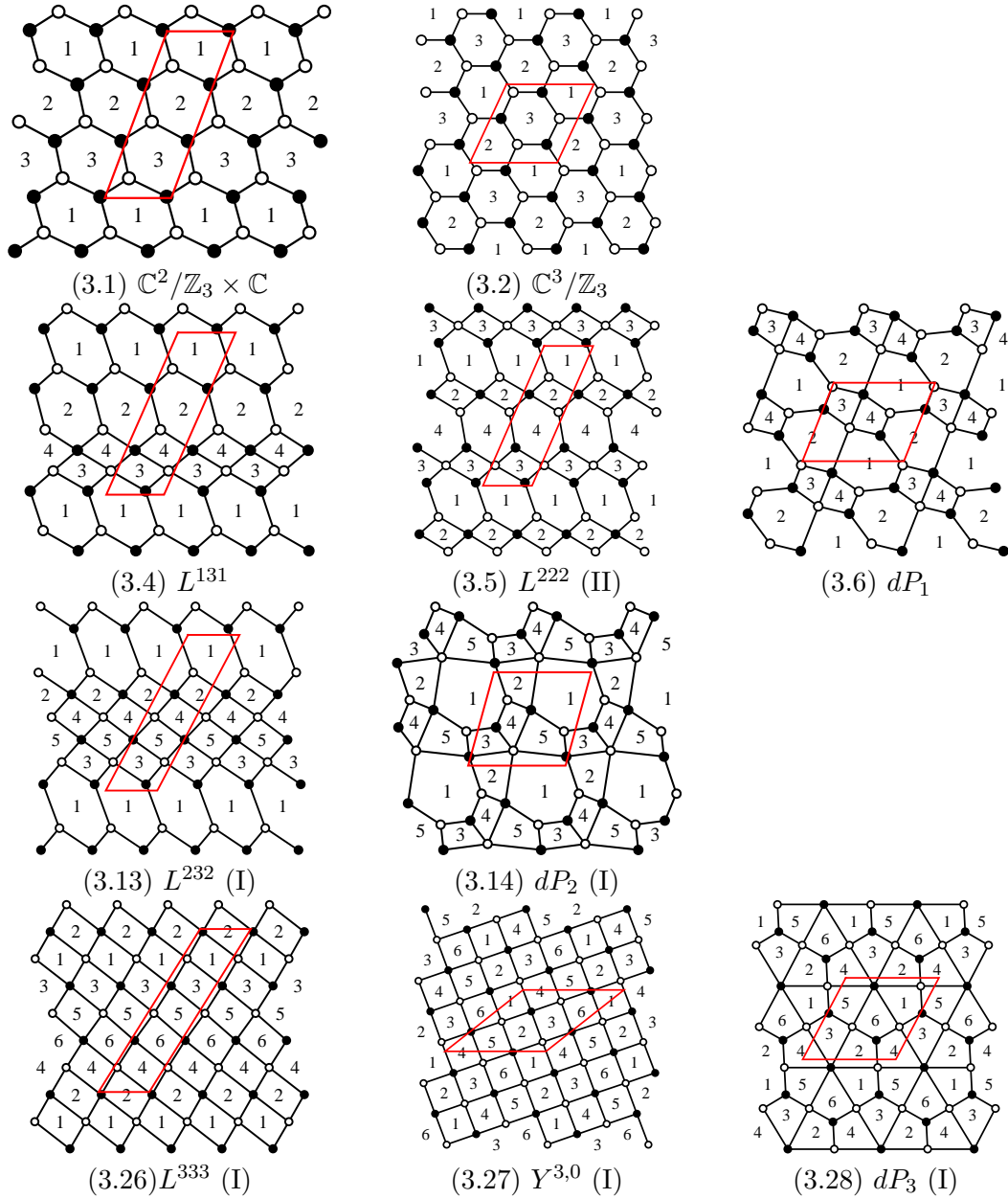


Figure 4.3.: Consistent tilings with six superpotential terms.

5. Conclusions

We have developed an algorithm to produce a list of possible brane tilings of up to six nodes, together with the associated moduli spaces. A key observation to simplify the classification task was the identification of “irreducible” quivers, corresponding to tilings with no multi-bonds. After restricting ourselves to irreducible models, we found that the number of tilings for each number of nodes N_T is finite. This allowed us to use N_T as the order parameter, and generate a full list of possible models for each considered value of N_T . The algorithm was efficient enough to produce all models with $N_T \leq 6$ in a couple of hours on a regular personal computer.

Among the tilings found we saw the models already known in the literature from analysis of D3 world-volume theories, such as dP_0, dP_1, dP_2, dP_3 , several cases from L^{aba} class. We have found no previously unknown tilings that would give a consistent (3+1) CFT, which is an assuring fact indicating that the space of consistent tilings is already explored well enough through studies of individual models. On the other hand, we found a lot of the so-called inconsistent tilings, which appear in the literature for the first time. The list in Appendix A thus provides a wealth of candidate models that can be explored in the context of M2 world-volume theories.

One natural extension of this work would be to attempt an even further classification of models. We believe the full lists for $N_T = 8$ and $N_T = 10$ should be attainable after some optimizations in the algorithm. An altogether different classification algorithm is also an option, possibly based on the idea of adding diagonals to obtain new tilings, as pointed out in the previous section. If this way we could bypass the generation of all the quiver gauge theories that do not admit a tiling description, it could provide a significant boost in efficiency.

Next, we can use the database of generated models to perform an inverse algorithm on backgrounds of interest, which was one of the main motivations of the work. One example of “interesting” backgrounds is the finite class of smooth toric Fano threefolds. An analysis of models dual to these surfaces was already started in [32], and it will be interesting to see if the process finding duals can be automated with the help of the current classification.

Another direction of further work could be to perform even more automatic

analysis on the generated models. This will no doubt be necessary in order to extract useful information, especially beyond $N_T = 8$, since the number of models will reach hundreds. For example, it would be tremendously useful to automatically calculate R-charges and Hilbert series for these models. We will have to see if that is possible.

Finally, we would like to make a public *Mathematica* package with implementation of all computations developed in the course of this work, so it can be further expanded, and used as a convenient tool to explore the space of brane tilings and toric geometry.

A. Appendix: Tiling catalog

In this appendix we give the details of all the tilings found by an implementation of the algorithm discussed in this paper. For each tiling we provide the quiver with the superpotential, the brane tiling and the corresponding toric diagram of the D3 brane theory. The conventional name of the model is included next to the toric diagram, and the “(inc.)” suffix indicates that the associated D3 brane theory is inconsistent. For models with a toric diagram which has more than one known phase we also include the phase number in parenthesis.

In each table for given order parameters we give the consistent models first, and then list the remaining tilings according to the area of their associated toric diagram.

A.1. Two superpotential terms

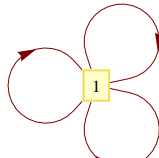
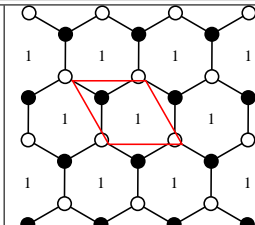
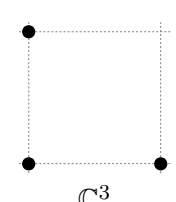

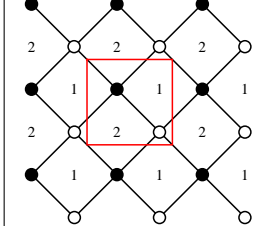
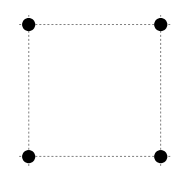
#	Quiver	Tiling	Toric Diagram	Superpotential
(1.1)			 \mathbb{C}^3	$\phi_1^1 \cdot \phi_1^2 \cdot \phi_1^3$ $-\phi_1^1 \cdot \phi_1^3 \cdot \phi_1^2$
(1.2)			 \mathcal{C}	$X_{12}^1 \cdot X_{21}^1 \cdot X_{12}^2 \cdot X_{21}^2$ $-X_{12}^1 \cdot X_{21}^2 \cdot X_{12}^2 \cdot X_{21}^1$

Table A.1.: Tilings with 2 superpotential terms

A.2. Four superpotential terms

#	Quiver	Tiling	Toric Diagram	Superpotential
(2.1)				$ \begin{aligned} & -X_{12}^1 \cdot \phi_2 \cdot X_{21}^1 \\ & +X_{12}^2 \cdot \phi_2 \cdot X_{21}^2 \\ & +\phi_1 \cdot X_{12}^1 \cdot X_{21}^1 \\ & -\phi_1 \cdot X_{12}^2 \cdot X_{21}^2 \end{aligned} $

Table A.2.: Tilings with 4 superpotential terms and 2 gauge groups

#	Quiver	Tiling	Toric Diagram	Superpotential
(2.2)				$ \begin{aligned} & \phi_1 \cdot X_{12} \cdot X_{21} \\ & -\phi_1 \cdot X_{13} \cdot X_{31} \\ & -X_{12} \cdot X_{23} \cdot X_{32} \cdot X_{21} \\ & +X_{13} \cdot X_{32} \cdot X_{23} \cdot X_{31} \end{aligned} $
(2.3)				$ \begin{aligned} & -X_{12}^1 \cdot X_{23}^2 \cdot X_{31}^1 \\ & +X_{12}^2 \cdot X_{23}^1 \cdot X_{31}^2 \\ & +\phi_1 \cdot X_{12}^1 \cdot X_{23}^1 \cdot X_{31}^1 \\ & -\phi_1 \cdot X_{12}^2 \cdot X_{23}^2 \cdot X_{31}^2 \end{aligned} $

Table A.3.: Tilings with 4 superpotential terms and 3 gauge groups

#	Quiver	Tiling	Toric Diagram	Superpotential
(2.4)			 $L^{222} \text{ (I)}$	$ \begin{aligned} & X_{12} \cdot X_{21} \cdot X_{13} \cdot X_{31} \\ & - X_{12} \cdot X_{24} \cdot X_{42} \cdot X_{21} \\ & - X_{13} \cdot X_{34} \cdot X_{43} \cdot X_{31} \\ & + X_{24} \cdot X_{43} \cdot X_{34} \cdot X_{42} \end{aligned} $
(2.5)			 $\mathbb{F}_0 \text{ (I)}$	$ \begin{aligned} & X_{12}^1 \cdot X_{23}^1 \cdot X_{34}^1 \cdot X_{41}^1 \\ & - X_{12}^1 \cdot X_{23}^2 \cdot X_{34}^1 \cdot X_{41}^2 \\ & - X_{12}^2 \cdot X_{23}^1 \cdot X_{34}^2 \cdot X_{41}^1 \\ & + X_{12}^2 \cdot X_{23}^2 \cdot X_{34}^2 \cdot X_{41}^2 \end{aligned} $
(2.6)			 $SPP \text{ (inc.)}$	$ \begin{aligned} & X_{12}^1 \cdot X_{23} \cdot X_{31} \\ & - X_{12}^1 \cdot X_{24} \cdot X_{41} \\ & - X_{12}^2 \cdot X_{23} \cdot X_{34} \cdot X_{43} \cdot X_{31} \\ & + X_{12}^2 \cdot X_{24} \cdot X_{43} \cdot X_{34} \cdot X_{41} \end{aligned} $

Table A.4.: Tilings with 4 superpotential terms and 4 gauge groups

A.3. Six superpotential terms

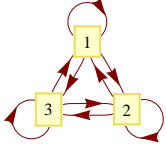
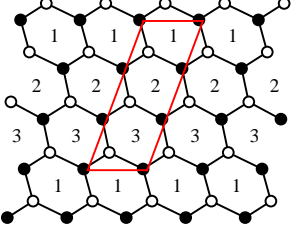
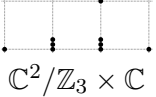
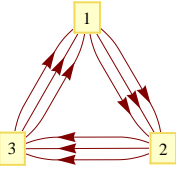
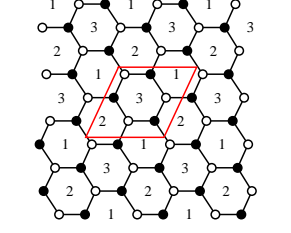
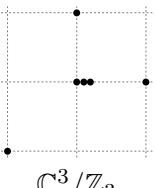
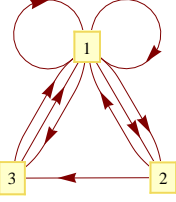
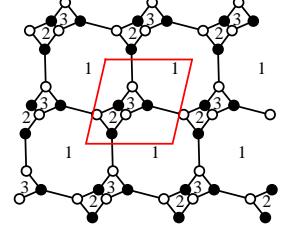
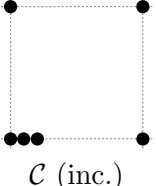
#	Quiver	Tiling	Toric Diagram	Superpotential
(3.1)			 $\mathbb{C}^2/\mathbb{Z}_3 \times \mathbb{C}$	$ \begin{aligned} & -X_{12} \cdot \phi_2 \cdot X_{21} \\ & +X_{13} \cdot \phi_3 \cdot X_{31} \\ & -X_{23} \cdot \phi_3 \cdot X_{32} \\ & +\phi_1 \cdot X_{12} \cdot X_{21} \\ & -\phi_1 \cdot X_{13} \cdot X_{31} \\ & +\phi_2 \cdot X_{23} \cdot X_{32} \end{aligned} $
(3.2)			 $\mathbb{C}^3/\mathbb{Z}_3$	$ \begin{aligned} & X_{12}^1 \cdot X_{23}^1 \cdot X_{31}^1 \\ & -X_{12}^1 \cdot X_{23}^3 \cdot X_{31}^2 \\ & -X_{12}^2 \cdot X_{23}^1 \cdot X_{31}^3 \\ & +X_{12}^2 \cdot X_{23}^2 \cdot X_{31}^2 \\ & -X_{12}^3 \cdot X_{23}^2 \cdot X_{31}^1 \\ & +X_{12}^3 \cdot X_{23}^3 \cdot X_{31}^3 \end{aligned} $
(3.3)			 $\mathcal{C} \text{ (inc.)}$	$ \begin{aligned} & -X_{12}^1 \cdot X_{23} \cdot X_{31}^1 \\ & +X_{12}^2 \cdot X_{23} \cdot X_{31}^2 \\ & +\phi_1^1 \cdot X_{12}^1 \cdot X_{21} \\ & -\phi_1^1 \cdot X_{13} \cdot X_{31}^2 \\ & -\phi_1^2 \cdot X_{12}^2 \cdot X_{21} \\ & +\phi_1^2 \cdot X_{13} \cdot X_{31}^1 \end{aligned} $

Table A.5.: Tilings with 6 superpotential terms and 3 gauge groups

#	Quiver	Tiling	Toric Diagram	Superpotential
(3.4)				$ \begin{aligned} & -X_{12} \cdot \phi_2 \cdot X_{21} \\ & + \phi_1 \cdot X_{12} \cdot X_{21} \\ & - \phi_1 \cdot X_{13} \cdot X_{31} \\ & + \phi_2 \cdot X_{24} \cdot X_{42} \\ & + X_{13} \cdot X_{34} \cdot X_{43} \cdot X_{31} \\ & - X_{24} \cdot X_{43} \cdot X_{34} \cdot X_{42} \end{aligned} $
(3.5)				$ \begin{aligned} & X_{24} \cdot \phi_4 \cdot X_{42} \\ & - X_{34} \cdot \phi_4 \cdot X_{43} \\ & + \phi_1 \cdot X_{12} \cdot X_{21} \\ & - \phi_1 \cdot X_{13} \cdot X_{31} \\ & - X_{12} \cdot X_{24} \cdot X_{42} \cdot X_{21} \\ & + X_{13} \cdot X_{34} \cdot X_{43} \cdot X_{31} \end{aligned} $
(3.6)				$ \begin{aligned} & X_{12}^1 \cdot X_{23}^1 \cdot X_{31} \\ & - X_{12}^1 \cdot X_{24} \cdot X_{41}^2 \\ & - X_{12}^2 \cdot X_{23}^2 \cdot X_{31} \\ & + X_{12}^2 \cdot X_{24} \cdot X_{41}^1 \\ & - X_{12}^3 \cdot X_{23}^1 \cdot X_{34} \cdot X_{41}^1 \\ & + X_{12}^3 \cdot X_{23}^2 \cdot X_{34} \cdot X_{41}^2 \end{aligned} $
(3.7)				$ \begin{aligned} & -X_{12} \cdot \phi_2 \cdot X_{21} \\ & + X_{13} \cdot X_{34}^1 \cdot X_{41} \\ & - X_{23} \cdot X_{34}^1 \cdot X_{42} \\ & + \phi_1 \cdot X_{12} \cdot X_{21} \\ & - \phi_1 \cdot X_{13} \cdot X_{34}^2 \cdot X_{41} \\ & + \phi_2 \cdot X_{23} \cdot X_{34}^2 \cdot X_{42} \end{aligned} $
(3.8)				$ \begin{aligned} & -X_{12}^1 \cdot X_{23} \cdot X_{31} \\ & + X_{12}^1 \cdot X_{24} \cdot X_{41}^1 \\ & - X_{13} \cdot X_{34} \cdot X_{41}^1 \\ & + \phi_1 \cdot X_{13} \cdot X_{31} \\ & + X_{12}^2 \cdot X_{23} \cdot X_{34} \cdot X_{41}^2 \\ & - \phi_1 \cdot X_{12}^2 \cdot X_{24} \cdot X_{41}^2 \end{aligned} $

Table A.6.: Tilings with 6 superpotential terms and 4 gauge groups (page 1/2)

#	Quiver	Tiling	Toric Diagram	Superpotential
(3.9)				$ \begin{aligned} & X_{12}^1 \cdot X_{23} \cdot X_{31} \\ & - X_{12}^1 \cdot X_{24} \cdot X_{41} \\ & + X_{13} \cdot X_{34} \cdot X_{41} \\ & - X_{23} \cdot X_{34} \cdot X_{42} \\ & - X_{12}^2 \cdot X_{21} \cdot X_{13} \cdot X_{31} \\ & + X_{12}^2 \cdot X_{24} \cdot X_{42} \cdot X_{21} \end{aligned} $
(3.10)				$ \begin{aligned} & - X_{12} \cdot X_{23}^2 \cdot X_{31} \\ & + X_{13} \cdot X_{34}^1 \cdot X_{41} \\ & - X_{23}^1 \cdot X_{34}^1 \cdot X_{42} \\ & + X_{23}^2 \cdot X_{34}^2 \cdot X_{42} \\ & + \phi_1 \cdot X_{12} \cdot X_{23}^1 \cdot X_{31} \\ & - \phi_1 \cdot X_{13} \cdot X_{34}^2 \cdot X_{41} \end{aligned} $
(3.11)				$ \begin{aligned} & - X_{13} \cdot X_{34} \cdot X_{41} \\ & - X_{14} \cdot X_{42} \cdot X_{21} \\ & + X_{23} \cdot X_{34} \cdot X_{42} \\ & + \phi_1 \cdot X_{14} \cdot X_{41} \\ & + X_{12} \cdot X_{21} \cdot X_{13} \cdot X_{31} \\ & - \phi_1 \cdot X_{12} \cdot X_{23} \cdot X_{31} \end{aligned} $
(3.12)				$ \begin{aligned} & X_{12}^1 \cdot X_{23} \cdot X_{31}^1 \\ & - X_{12}^2 \cdot X_{23} \cdot X_{31}^2 \\ & - X_{14}^1 \cdot X_{43} \cdot X_{31}^1 \\ & + X_{14}^2 \cdot X_{43} \cdot X_{31}^2 \\ & - X_{12}^1 \cdot X_{21} \cdot X_{14}^2 \cdot X_{41} \\ & + X_{12}^2 \cdot X_{21} \cdot X_{14}^1 \cdot X_{41} \end{aligned} $

Table A.7.: Tilings with 6 superpotential terms and 4 gauge groups (page 2/2)

#	Quiver	Tiling	Toric Diagram	Superpotential
(3.13)				$\begin{aligned} & \phi_1 \cdot X_{12} \cdot X_{21} \\ & - \phi_1 \cdot X_{13} \cdot X_{31} \\ & - X_{12} \cdot X_{24} \cdot X_{42} \cdot X_{21} \\ & + X_{13} \cdot X_{35} \cdot X_{53} \cdot X_{31} \\ & + X_{24} \cdot X_{45} \cdot X_{54} \cdot X_{42} \\ & - X_{35} \cdot X_{54} \cdot X_{45} \cdot X_{53} \end{aligned}$
(3.14)				$\begin{aligned} & X_{12}^1 \cdot X_{24} \cdot X_{41} \\ & - X_{13} \cdot X_{34} \cdot X_{41} \\ & + X_{13} \cdot X_{35} \cdot X_{51}^2 \\ & - X_{12}^1 \cdot X_{23} \cdot X_{35} \cdot X_{51}^1 \\ & - X_{12}^2 \cdot X_{24} \cdot X_{45} \cdot X_{51}^2 \\ & + X_{12}^2 \cdot X_{23} \cdot X_{34} \cdot X_{45} \cdot X_{51}^1 \end{aligned}$
(3.15)				$\begin{aligned} & X_{14} \cdot X_{45}^1 \cdot X_{51} \\ & - X_{34} \cdot X_{45}^1 \cdot X_{53} \\ & + \phi_1 \cdot X_{12} \cdot X_{21} \\ & - X_{12} \cdot X_{23} \cdot X_{32} \cdot X_{21} \\ & - \phi_1 \cdot X_{14} \cdot X_{45}^2 \cdot X_{51} \\ & + X_{23} \cdot X_{34} \cdot X_{45}^2 \cdot X_{53} \cdot X_{32} \end{aligned}$
(3.16)				$\begin{aligned} & X_{23} \cdot X_{34}^2 \cdot X_{42} \\ & - X_{34}^2 \cdot X_{45} \cdot X_{53} \\ & + \phi_1 \cdot X_{12} \cdot X_{21} \\ & - \phi_1 \cdot X_{15} \cdot X_{51} \\ & - X_{12} \cdot X_{23} \cdot X_{34}^1 \cdot X_{42} \cdot X_{21} \\ & + X_{15} \cdot X_{53} \cdot X_{34}^1 \cdot X_{45} \cdot X_{51} \end{aligned}$
(3.17)				$\begin{aligned} & - X_{13} \cdot X_{34} \cdot X_{41} \\ & + X_{13} \cdot X_{35} \cdot X_{51} \\ & - X_{14} \cdot X_{45} \cdot X_{51} \\ & + X_{12} \cdot X_{21} \cdot X_{14} \cdot X_{41} \\ & + X_{23} \cdot X_{34} \cdot X_{45} \cdot X_{52} \\ & - X_{12} \cdot X_{23} \cdot X_{35} \cdot X_{52} \cdot X_{21} \end{aligned}$

Table A.8.: Tilings with 6 superpotential terms and 5 gauge groups (page 1/3)

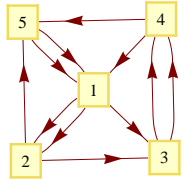
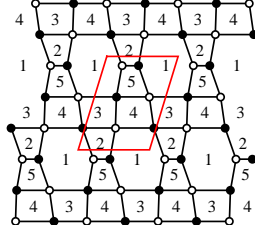
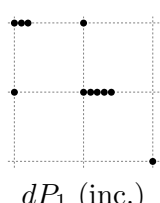
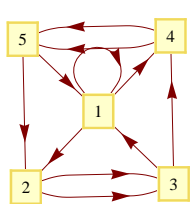
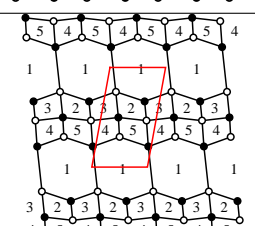
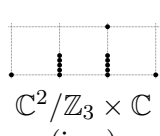
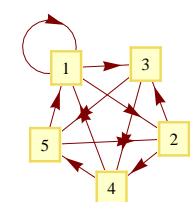
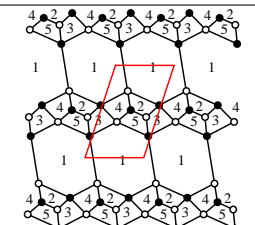
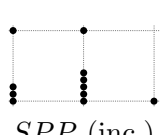
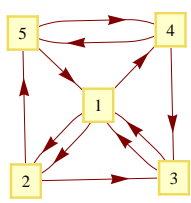
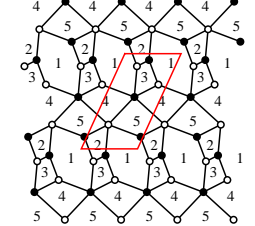
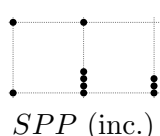
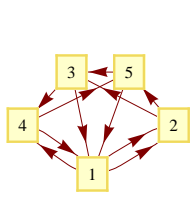
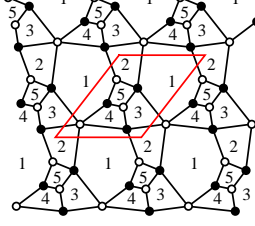
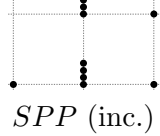
#	Quiver	Tiling	Toric Diagram	Superpotential
(3.18)			 dP_1 (inc.)	$ \begin{aligned} & X_{12}^1 \cdot X_{25} \cdot X_{51}^1 \\ & - X_{12}^2 \cdot X_{25} \cdot X_{51}^2 \\ & - X_{12}^1 \cdot X_{23} \cdot X_{34}^2 \cdot X_{41} \\ & + X_{12}^2 \cdot X_{23} \cdot X_{34}^1 \cdot X_{41} \\ & - X_{13} \cdot X_{34}^1 \cdot X_{45} \cdot X_{51}^1 \\ & + X_{13} \cdot X_{34}^2 \cdot X_{45} \cdot X_{51}^2 \end{aligned} $
(3.19)			 $\mathbb{C}^2/\mathbb{Z}_3 \times \mathbb{C}$ (inc.)	$ \begin{aligned} & - X_{12} \cdot X_{23}^2 \cdot X_{31} \\ & + X_{14} \cdot X_{45}^1 \cdot X_{51} \\ & - X_{23}^1 \cdot X_{34} \cdot X_{45}^1 \cdot X_{52} \\ & + X_{23}^2 \cdot X_{34} \cdot X_{45}^2 \cdot X_{52} \\ & + \phi_1 \cdot X_{12} \cdot X_{23}^1 \cdot X_{31} \\ & - \phi_1 \cdot X_{14} \cdot X_{45}^2 \cdot X_{51} \end{aligned} $
(3.20)			 SPP (inc.)	$ \begin{aligned} & X_{23} \cdot X_{35} \cdot X_{52} \\ & - X_{24} \cdot X_{45} \cdot X_{52} \\ & - X_{12} \cdot X_{23} \cdot X_{34} \cdot X_{41} \\ & + X_{13} \cdot X_{34} \cdot X_{45} \cdot X_{51} \\ & + \phi_1 \cdot X_{12} \cdot X_{24} \cdot X_{41} \\ & - \phi_1 \cdot X_{13} \cdot X_{35} \cdot X_{51} \end{aligned} $
(3.21)			 SPP (inc.)	$ \begin{aligned} & X_{12}^1 \cdot X_{23} \cdot X_{31}^1 \\ & - X_{12}^1 \cdot X_{25} \cdot X_{51} \\ & - X_{12}^2 \cdot X_{23} \cdot X_{31}^2 \\ & + X_{14} \cdot X_{43} \cdot X_{31}^1 \\ & + X_{12}^2 \cdot X_{25} \cdot X_{54} \cdot X_{45} \cdot X_{51} \\ & - X_{14} \cdot X_{45} \cdot X_{54} \cdot X_{43} \cdot X_{31}^1 \end{aligned} $
(3.22)			 SPP (inc.)	$ \begin{aligned} & X_{12}^1 \cdot X_{25} \cdot X_{51} \\ & - X_{14} \cdot X_{45} \cdot X_{51} \\ & + X_{34} \cdot X_{45} \cdot X_{53} \\ & - X_{12}^1 \cdot X_{23} \cdot X_{34} \cdot X_{41} \\ & - X_{12}^2 \cdot X_{25} \cdot X_{53} \cdot X_{31} \\ & + X_{12}^2 \cdot X_{23} \cdot X_{31} \cdot X_{14} \cdot X_{41} \end{aligned} $

Table A.9.: Tilings with 6 superpotential terms and 5 gauge groups (page 2/3)

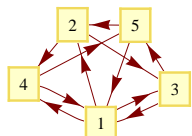
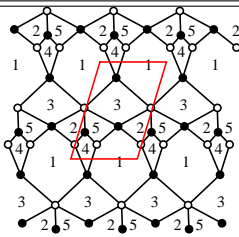
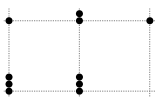
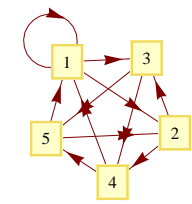
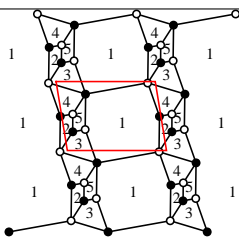
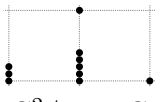
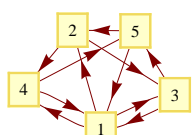
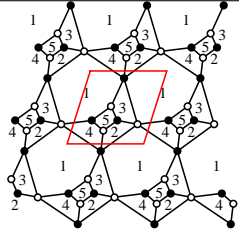
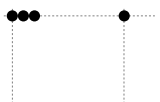
#	Quiver	Tiling	Toric Diagram	Superpotential
(3.23)			 <i>SPP</i> (inc.)	$ \begin{aligned} & X_{12} \cdot X_{24} \cdot X_{41} \\ & + X_{14} \cdot X_{45} \cdot X_{51} \\ & - X_{24} \cdot X_{45} \cdot X_{52} \\ & - X_{12} \cdot X_{23} \cdot X_{35} \cdot X_{51} \\ & - X_{13} \cdot X_{31} \cdot X_{14} \cdot X_{41} \\ & + X_{13} \cdot X_{35} \cdot X_{52} \cdot X_{23} \cdot X_{31} \end{aligned} $
(3.24)			 $\mathbb{C}^2/\mathbb{Z}_2 \times \mathbb{C}$ (inc.)	$ \begin{aligned} & - X_{12} \cdot X_{24} \cdot X_{41} \\ & + X_{13} \cdot X_{35} \cdot X_{51} \\ & - X_{23} \cdot X_{35} \cdot X_{52} \\ & + X_{24} \cdot X_{45} \cdot X_{52} \\ & + \phi_1 \cdot X_{12} \cdot X_{23} \cdot X_{34} \cdot X_{41} \\ & - \phi_1 \cdot X_{13} \cdot X_{34} \cdot X_{45} \cdot X_{51} \end{aligned} $
(3.25)			 \mathcal{C} (inc.)	$ \begin{aligned} & X_{13} \cdot X_{35} \cdot X_{51} \\ & - X_{14} \cdot X_{45} \cdot X_{51} \\ & - X_{23} \cdot X_{35} \cdot X_{52} \\ & + X_{24} \cdot X_{45} \cdot X_{52} \\ & + X_{12} \cdot X_{23} \cdot X_{31} \cdot X_{14} \cdot X_{41} \\ & - X_{12} \cdot X_{24} \cdot X_{41} \cdot X_{13} \cdot X_{31} \end{aligned} $

Table A.10.: Tilings with 6 superpotential terms and 5 gauge groups (**page 3/3**)

#	Quiver	Tiling	Toric Diagram	Superpotential
(3.26)				$ \begin{aligned} & X_{12} \cdot X_{21} \cdot X_{13} \cdot X_{31} \\ & - X_{12} \cdot X_{24} \cdot X_{42} \cdot X_{21} \\ & - X_{13} \cdot X_{35} \cdot X_{53} \cdot X_{31} \\ & + X_{24} \cdot X_{46} \cdot X_{64} \cdot X_{42} \\ & + X_{35} \cdot X_{56} \cdot X_{65} \cdot X_{53} \\ & - X_{46} \cdot X_{65} \cdot X_{56} \cdot X_{64} \end{aligned} $
(3.27)				$ \begin{aligned} & X_{12}^1 \cdot X_{23} \cdot X_{34}^1 \cdot X_{41} \\ & - X_{12}^1 \cdot X_{25} \cdot X_{56}^2 \cdot X_{61} \\ & - X_{12}^2 \cdot X_{23} \cdot X_{34}^2 \cdot X_{41} \\ & + X_{12}^2 \cdot X_{25} \cdot X_{56}^1 \cdot X_{61} \\ & - X_{34}^1 \cdot X_{45} \cdot X_{56}^1 \cdot X_{63} \\ & + X_{34}^2 \cdot X_{45} \cdot X_{56}^2 \cdot X_{63} \end{aligned} $
(3.28)				$ \begin{aligned} & - X_{13} \cdot X_{35} \cdot X_{51} \\ & - X_{24} \cdot X_{46} \cdot X_{62} \\ & + X_{12} \cdot X_{24} \cdot X_{45} \cdot X_{51} \\ & + X_{13} \cdot X_{34} \cdot X_{46} \cdot X_{61} \\ & + X_{23} \cdot X_{35} \cdot X_{56} \cdot X_{62} \\ & - X_{12} \cdot X_{23} \cdot X_{34} \cdot X_{45} \cdot X_{56} \cdot X_{61} \end{aligned} $
(3.29)				$ \begin{aligned} & X_{34} \cdot X_{46} \cdot X_{63} \\ & - X_{35} \cdot X_{56} \cdot X_{63} \\ & + X_{12}^1 \cdot X_{23} \cdot X_{35} \cdot X_{51} \\ & - X_{12}^1 \cdot X_{24} \cdot X_{46} \cdot X_{61} \\ & - X_{12}^2 \cdot X_{23} \cdot X_{34} \cdot X_{45} \cdot X_{51} \\ & + X_{12}^2 \cdot X_{24} \cdot X_{45} \cdot X_{56} \cdot X_{61} \end{aligned} $
(3.30)				$ \begin{aligned} & X_{12}^1 \cdot X_{23} \cdot X_{31} \\ & - X_{12}^1 \cdot X_{24} \cdot X_{41} \\ & + X_{35} \cdot X_{56} \cdot X_{65} \cdot X_{53} \\ & - X_{46} \cdot X_{65} \cdot X_{56} \cdot X_{64} \\ & - X_{12}^2 \cdot X_{23} \cdot X_{35} \cdot X_{53} \cdot X_{31} \\ & + X_{12}^2 \cdot X_{24} \cdot X_{46} \cdot X_{64} \cdot X_{41} \end{aligned} $

Table A.11.: Tilings with 6 superpotential terms and 6 gauge groups (page 1/3)

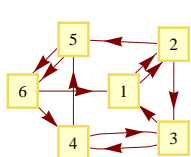
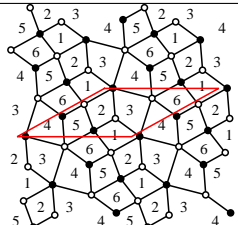
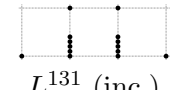
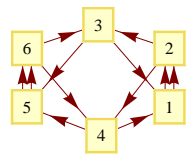
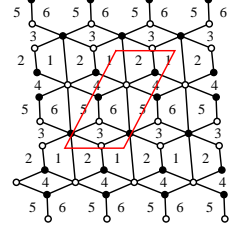
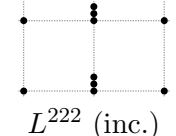
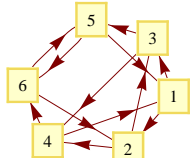
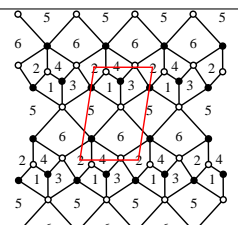
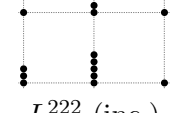
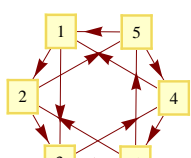
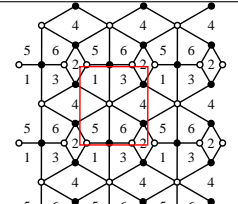

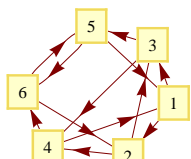
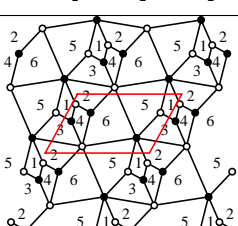

#	Quiver	Tiling	Toric Diagram	Superpotential
(3.31)				$ \begin{aligned} & X_{12}^1 \cdot X_{23} \cdot X_{31} \\ & - X_{45} \cdot X_{56}^1 \cdot X_{64} \\ & - X_{12}^1 \cdot X_{25} \cdot X_{56}^2 \cdot X_{61} \\ & + X_{12}^2 \cdot X_{25} \cdot X_{56}^1 \cdot X_{61} \\ & - X_{12}^2 \cdot X_{23} \cdot X_{34} \cdot X_{43} \cdot X_{31} \\ & + X_{34} \cdot X_{45} \cdot X_{56}^2 \cdot X_{64} \cdot X_{43} \end{aligned} $
(3.32)				$ \begin{aligned} & X_{12}^1 \cdot X_{23} \cdot X_{31} \\ & - X_{12}^1 \cdot X_{24} \cdot X_{41} \\ & + X_{35} \cdot X_{56}^2 \cdot X_{63} \\ & - X_{45} \cdot X_{56}^1 \cdot X_{64} \\ & - X_{12}^2 \cdot X_{23} \cdot X_{35} \cdot X_{56}^1 \cdot X_{63} \cdot X_{31} \\ & + X_{12}^2 \cdot X_{24} \cdot X_{45} \cdot X_{56}^1 \cdot X_{64} \cdot X_{41} \end{aligned} $
(3.33)				$ \begin{aligned} & X_{12} \cdot X_{24} \cdot X_{41} \\ & - X_{13} \cdot X_{34} \cdot X_{41} \\ & - X_{12} \cdot X_{23} \cdot X_{35} \cdot X_{51} \\ & + X_{23} \cdot X_{34} \cdot X_{46} \cdot X_{62} \\ & + X_{13} \cdot X_{35} \cdot X_{56} \cdot X_{65} \cdot X_{51} \\ & - X_{24} \cdot X_{46} \cdot X_{65} \cdot X_{56} \cdot X_{62} \end{aligned} $
(3.34)				$ \begin{aligned} & X_{12} \cdot X_{25} \cdot X_{51} \\ & + X_{23} \cdot X_{36} \cdot X_{62} \\ & - X_{12} \cdot X_{23} \cdot X_{34} \cdot X_{41} \\ & - X_{13} \cdot X_{36} \cdot X_{65} \cdot X_{51} \\ & - X_{25} \cdot X_{54} \cdot X_{46} \cdot X_{62} \\ & + X_{13} \cdot X_{34} \cdot X_{46} \cdot X_{65} \cdot X_{54} \cdot X_{41} \end{aligned} $
(3.35)				$ \begin{aligned} & X_{12} \cdot X_{24} \cdot X_{41} \\ & - X_{13} \cdot X_{34} \cdot X_{41} \\ & + X_{13} \cdot X_{35} \cdot X_{51} \\ & - X_{24} \cdot X_{46} \cdot X_{62} \\ & - X_{12} \cdot X_{23} \cdot X_{35} \cdot X_{56} \cdot X_{65} \cdot X_{51} \\ & + X_{23} \cdot X_{34} \cdot X_{46} \cdot X_{65} \cdot X_{56} \cdot X_{62} \end{aligned} $

Table A.12.: Tilings with 6 superpotential terms and 6 gauge groups (page 2/3)

#	Quiver	Tiling	Toric Diagram	Superpotential
(3.36)			 <i>SPP</i> (inc.)	$ \begin{aligned} & X_{12} \cdot X_{25} \cdot X_{51} \\ & + X_{23} \cdot X_{36} \cdot X_{62} \\ & - X_{25} \cdot X_{56} \cdot X_{62} \\ & - X_{12} \cdot X_{23} \cdot X_{34} \cdot X_{41} \\ & - X_{13} \cdot X_{36} \cdot X_{64} \cdot X_{45} \cdot X_{51} \\ & + X_{13} \cdot X_{34} \cdot X_{45} \cdot X_{56} \cdot X_{64} \cdot X_{41} \end{aligned} $
(3.37)			 \mathcal{C} (inc.)	$ \begin{aligned} & - X_{23} \cdot X_{36} \cdot X_{62} \\ & + X_{25} \cdot X_{56} \cdot X_{62} \\ & + X_{36} \cdot X_{64} \cdot X_{43} \\ & - X_{45} \cdot X_{56} \cdot X_{64} \\ & + X_{12} \cdot X_{23} \cdot X_{31} \cdot X_{14} \cdot X_{45} \cdot X_{51} \\ & - X_{12} \cdot X_{25} \cdot X_{51} \cdot X_{14} \cdot X_{43} \cdot X_{31} \end{aligned} $

Table A.13.: Tilings with 6 superpotential terms and 6 gauge groups (**page 3/3**)

Bibliography

- [1] J. Davey, A. Hanany and J. Pasukonis, “On the Classification of Brane Tilings,” arXiv:0909.2868 [hep-th].
- [2] A. Hanany and K. D. Kennaway, “Dimer models and toric diagrams,” arXiv:hep-th/0503149.
- [3] S. Franco, A. Hanany, K. D. Kennaway, D. Vegh and B. Wecht, “Brane Dimers and Quiver Gauge Theories,” JHEP **0601** (2006) 096 [arXiv:hep-th/0504110].
- [4] K. D. Kennaway, “Brane Tilings,” Int. J. Mod. Phys. A **22** (2007) 2977 [arXiv:0706.1660 [hep-th]].
- [5] M. Yamazaki, “Brane Tilings and Their Applications,” Fortsch. Phys. **56** (2008) 555 [arXiv:0803.4474 [hep-th]].
- [6] J. Bagger and N. Lambert, “Modeling multiple M2’s,” Phys. Rev. D **75**, 045020 (2007) [arXiv:hep-th/0611108]. “Gauge Symmetry and Supersymmetry of Multiple M2-Branes,” Phys. Rev. D **77**, 065008 (2008) [arXiv:0711.0955 [hep-th]]. “Comments On Multiple M2-branes,” JHEP **0802**, 105 (2008) [arXiv:0712.3738 [hep-th]].
- [7] A. Gustavsson, “Algebraic structures on parallel M2-branes,” arXiv:0709.1260 [hep-th]. “Selfdual strings and loop space Nahm equations,” JHEP **0804**, 083 (2008) [arXiv:0802.3456 [hep-th]].
- [8] O. Aharony, O. Bergman, D. L. Jafferis and J. Maldacena, “N=6 superconformal Chern-Simons-matter theories, M2-branes and their gravity duals,” arXiv:0806.1218 [hep-th].
- [9] A. Hanany and A. Zaffaroni, “Tilings, Chern-Simons Theories and M2 Branes,” JHEP **0810** (2008) 111 [arXiv:0808.1244 [hep-th]].
- [10] A. Hanany, D. Vegh and A. Zaffaroni, “Brane Tilings and M2 Branes,” JHEP **0903** (2009) 012 [arXiv:0809.1440 [hep-th]].

- [11] A. Hanany and Y. H. He, “M2-Branes and Quiver Chern-Simons: A Taxonomic Study,” arXiv:0811.4044 [hep-th].
- [12] A. Kehagias, “New Type IIB vacua and their F-theory interpretation,” Phys. Lett. B **435** (1998) 337 [arXiv:hep-th/9805131].
- [13] I. R. Klebanov and E. Witten, “Superconformal field theory on threebranes at a Calabi-Yau singularity,” Nucl. Phys. B **536** (1998) 199 [arXiv:hep-th/9807080].
- [14] B. S. Acharya, J. M. Figueroa-O’Farrill, C. M. Hull and B. J. Spence, “Branes at conical singularities and holography,” Adv. Theor. Math. Phys. **2** (1999) 1249 [arXiv:hep-th/9808014].
- [15] D. R. Morrison and M. R. Plesser, “Non-spherical horizons. I,” Adv. Theor. Math. Phys. **3** (1999) 1 [arXiv:hep-th/9810201].
- [16] A. Hanany and D. Vegh, “Quivers, tilings, branes and rhombi,” JHEP **0710** (2007) 029 [arXiv:hep-th/0511063].
- [17] S. Franco, A. Hanany, J. Park and D. Rodriguez-Gomez, “Towards M2-brane Theories for Generic Toric Singularities,” JHEP **0812** (2008) 110 [arXiv:0809.3237 [hep-th]].
- [18] B. Feng, S. Franco, A. Hanany and Y. H. He, “Symmetries of toric duality,” JHEP **0212** (2002) 076 [arXiv:hep-th/0205144].
- [19] A. Hanany, P. Kazakopoulos and B. Wecht, “A new infinite class of quiver gauge theories,” JHEP **0508** (2005) 054 [arXiv:hep-th/0503177].
- [20] T. Oota and Y. Yasui, “New example of infinite family of quiver gauge theories,” Nucl. Phys. B **762** (2007) 377 [arXiv:hep-th/0610092].
- [21] M. Cvetič, H. Lu, D. N. Page and C. N. Pope, “New Einstein-Sasaki spaces in five and higher dimensions,” Phys. Rev. Lett. **95** (2005) 071101 [arXiv:hep-th/0504225].
- [22] B. Feng, A. Hanany and Y. H. He, “D-brane gauge theories from toric singularities and toric duality,” Nucl. Phys. B **595** (2001) 165 [arXiv:hep-th/0003085].
- [23] B. Feng, Y. H. He and F. Lam, “On correspondences between toric singularities and (p,q)-webs,” Nucl. Phys. B **701** (2004) 334 [arXiv:hep-th/0403133].

- [24] K. A. Intriligator and B. Wecht, “The exact superconformal R-symmetry maximizes a,” Nucl. Phys. B **667** (2003) 183 [arXiv:hep-th/0304128].
- [25] D. Kutasov, “New results on the ‘a-theorem’ in four dimensional supersymmetric field theory,” arXiv:hep-th/0312098.
- [26] P. S. Aspinwall and I. V. Melnikov, “D-branes on vanishing del Pezzo surfaces,” JHEP **0412** (2004) 042 [arXiv:hep-th/0405134].
- [27] B. Feng, A. Hanany, Y. H. He and A. Iqbal, “Quiver theories, soliton spectra and Picard-Lefschetz transformations,” JHEP **0302** (2003) 056 [arXiv:hep-th/0206152].
- [28] C. P. Herzog, “Seiberg duality is an exceptional mutation,” JHEP **0408** (2004) 064 [arXiv:hep-th/0405118].
- [29] D. R. Gulotta, “Properly ordered dimers, R -charges, and an efficient inverse algorithm,” JHEP **0810** (2008) 014 [arXiv:0807.3012 [hep-th]].
- [30] J. Davey, A. Hanany, N. Mekareeya and G. Torri, “Phases of M2-brane Theories,” JHEP **0906** (2009) 025 [arXiv:0903.3234 [hep-th]].
- [31] W. Fulton, “Introduction to Toric Varieties,” Princeton University Press, 1993.
- [32] A. Hanany and Y. H. He, “Chern-Simons: Fano and Calabi-Yau,” arXiv:0904.1847 [hep-th].